Frey, F.A., Coffin, M.F., Wallace, P.J., and Quilty, P.G. (Eds.)
Proceedings of the Ocean Drilling Program, Scientific Results Volume 183

15. Data Report: Alteration of Basalts from the Kerguelen Plateau[1]

V. Kurnosov,[2] B. Zolotarev,[2] A. Artamonov,[2] S. Garanina,[2]
V. Petrova,[2] V. Eroshchev-Shak,[2] and A. Sokolova[2]

ABSTRACT

The basalts recovered during Legs 183 and 120 from the southern, central, and northernmost parts of the Kerguelen Plateau (Holes 1136A, 1138A, 1140A, and 747C, respectively), as well as those recovered from the eastern part of the crest of Elan Bank (Hole 1137A), represent derivates from tholeiitic melts. In the northern part of the Kerguelen Plateau (Hole 1140A), basalts may have formed from two sources located at different depths. This is reflected in the presence of both low- and high-titanium basalts.

The basalts are variably altered by low-temperature hydrothermal processes (at temperatures up to 120°C), and some are affected by subaerial weathering. The hydrothermal alteration led mainly to the formation of smectites, chlorite minerals, mixed-layer hydromica-smectite and smectite-chlorite minerals, hydromica, serpentine(?), clinoptilolite, heulandite, stilbite, analcime, mordenite, thomsonite, natrolite(?), calcite, quartz, and dickite(?). Alteration of extrusive basalts is mainly related to horizontal fluid flow within permeable contact zones between lava flows. Under a nonoxidizing environment of alteration, the tendency to lose most of elements, including rare earth elements, from basalts dominates. Under on oxidizing environment, basalts accumulate many elements.

INTRODUCTION

Basalts from aseismic structures and guyots and their alteration are less studied than those from mid-ocean ridges. Aseismic ridges and pla-

[1]Kurnosov, V., Zolotarev, B., Artamonov, A., Garanina, S., Petrova, V., Eroshchev-Shak, V., and Sokolova, A., 2003. Data report: Alteration of basalts from the Kerguelen Plateau. *In* Frey, F.A., Coffin, M.F., Wallace, P.J., and Quilty, P.G. (Eds.), *Proc. ODP, Sci. Results,* 183, 1–40 [Online]. Available from World Wide Web: <http://www-odp.tamu.edu/publications/183_SR/VOLUME/CHAPTERS/013.PDF>. [Cited YYYY-MM-DD]
[2]Geological Institute, Russian Academy of Sciences, Pyzhevsky Lane 7, Moscow 109017, Russian Federation. Correspondence author: **kurnosov@geo.tv-sign.ru**

Initial receipt: 26 February 2002
Acceptance: 19 October 2002
Web publication: 1 April 2003
Ms 183SR-013

teaus represent giant structures on the ocean floor that are often linear and extend several thousand kilometers to form large igneous provinces (LIPs). These structures reveal the characteristic features of magma composition, extrusion environment (from shallow-water and subaerial to deepwater environments), thermal history, and circulation of both seawater and meteoric fluids (Kurnosov et al., 1995; Kurnosov and Murdmaa, 1996). Variation in tectonic setting during the formation of these volcanic structures leads to significant variation in chemical composition of lava flows and pillow units (Vallier et al., 1981).

The combination of these peculiarities for aseismic ridges and plateaus is somewhat specific in comparison to mid-ocean ridges. Therefore, alteration of basalts in these structures generates characteristic features that need further investigation. Study of basalt alteration requires analyses of thin sections, chemical composition of both altered rocks and their protoliths, densities, and alteration of secondary minerals. We used this approach during the study of basalts recovered from Holes 1136A, 1137A, 1138A, and 1140A (Leg 183) and from Hole 747C (Leg 120) from various parts of the Kerguelen Plateau.

In this article, we have determined

1. Petrography, chemical composition, and densities of fresh and altered volcanic rocks and
2. Secondary minerals and chemical changes in altered basalts.

METHODS

For this article, we performed the following analyses:

The study of both petrographic and chemical compositions of unaltered and altered rocks,
The study of secondary mineral assemblages,
The determination of densities of fresh and altered rocks, and
The calculation of atoms of each element in a standard volume of both fresh and altered rocks (grams per 1000 cm^3 of rock) on the basis of the atomic-volumetric method of recalculation of chemical analyses with correction for porosity.

All analyses were conducted at the Geological Institute, Russian Academy of Sciences.

Petrography, X-Ray Diffraction, and Microprobe Analysis

Altered and fresh basalts were studied in thin section in order to determine their mineralogy. Secondary minerals from igneous rocks were studied in thin section and examined by X-ray diffraction (XRD) and microprobe analysis.

Prior to XRD analyses, any specimens with clay minerals were air-dried, treated with glycerol or, in part, with ethylene glycol, and heated at 550°C for 1 hr. A DRON-3 X-ray diffractometer with CuK_α emission, Ni filter, and slit widths of 0.5, 1, 1, and 0.5 mm was used to analyze the specimens. We examined secondary minerals in basalts from vesicles and veins by XRD. In addition, specimens were prepared from suspensions using distilled water and basalt pieces were ground to 1–2 mm in an agate mortar. Clay minerals were concentrated in suspensions.

Density Analysis

We determined the density of igneous rocks by weighing the samples using an analytical balance with a precision of 0.001 g. The routine method included (1) weighing the sample after drying at temperatures from 105° to 110°C, (2) plunging the sample in melted paraffin at 60°C, and (3) weighing the paraffined sample in both air and water.

Wet Chemical Analysis

Major elements in bulk samples of igneous rocks were analyzed by "classical" wet chemistry. This included the determination of H_2O^+, H_2O^-, Fe_2O_3, FeO, and CO_2.

X-Ray Fluorescence and Atomic Emission Spectroscopy Analyses

To determine trace elements, we used both atomic emission spectroscopy (AES) for Cr, Ni, Co, V, Cu, Pb, and Zn and X-ray fluorescence (XRF) analysis for Y, Nb, Rb, Sr, Zr, and Ba.

Rare Earth Element Analysis

Rare earth elements (REEs) in igneous rocks were determined by radiochemical neutron activation. Samples (100 mg each) were irradiated together with a standard by thermal neutron flux of 1.2×10^{13} n/cm^{2}s over 20 hr. REE fractions were separated radiochemically. Gamma spectrometry determination of REEs was by coaxial Ge (Li) detector. The accuracy of the analysis (1-σ error) for individual elements is ±3%–5% for La, Sm, Eu, and Yb; ±5%–7% for Ce and Tb; and ±10% for Nd. The accuracy of the determination has been checked against the U.S. Geologic Survey BHVO-1 standard reference material (Gladney and Roelandts, 1988).

Atomic Volume Method for Recalculation of Chemical Data

We used the atomic volume system for recalculation of chemical data as the preferred method for determination of gain/loss of matter during alteration of igneous rocks (Kurnosov, 1986). The procedures for these calculations are described by Kazitzyn and Rudnik (1968).

This method aims to show components of rocks in atomic form in some standard volume and requires recalculation of chemical analyses with due regard for porosity and real packing of atoms in minerals. The atomic content of each element can be quantified in grams per standard volume.

To estimate the mass balance resulting from metasomatic processes, calculations have to be based on geometric volumes (i.e., with due regard to the porosity of the rock). A greater percentage composition (in weight percent) of matter does not necessarily correspond to greater absolute content in the rock.

To avoid gross errors during the determination of gain/loss of matter, it is necessary be sure that the protolith has been accurately identified. Collection of such samples is very complex.

Comparison of massive and vesicular basalt samples within one group may result in a gross error. Vesicular basalts are widespread in seamounts. Altered vesicular basalts and especially highly vesicular basalts have less element per unit volume before alteration than massive basalts.

We recalculated chemical data using the following formula (Kazitzyn and Rudnik, 1968):

$$P_i = 0.166 \times a_i \times P_o^{\,i} \times d_v \times R_o, \quad (1)$$

where

P_i = content of element (grams) in 1000 cm^3 of rock;
a_i = atomic weight of element;
$P_o^{\,i}$ = value of element in the oxidized form (weight percent);
d_v = density of the sample (grams per cubic centimeters); and
R_o = transitional coefficient for each oxide (Table T1).

T1. Transitional coefficient R_o, p. 19.

We excluded H_2O^- from chemical analyses and recalculated results to 100%.

We simplified these calculations for oxides by replacing the constant ($0.166 \times a_i \times R_o$) for each oxide with coefficient K (Table T2). Thus,

T2. Coefficient K, p. 20.

$$P_i = K \times P_o^{\,i} \times d_v. \quad (2)$$

To calculate the abundance of a chemical elements (grams) in 1000 cm^3 of rock, if it is determined in weight percent, one can use equation 1 or 2. The transitional coefficient R can be calculated as

$$R = (1000{:}6.6){:}a_i \text{ or}$$

$$R = 60.241{:}a_i,$$

where a_i = atomic weight of an element.

The content of a trace element is given in parts per million (grams per ton [g/ton] of rock):

$$P_i = P_a^{\,i} \times d_v \times 10^{-3}, \quad (3)$$

where

P_i = content of element (grams) in 1000 cm^3 of rock;
$P_a^{\,i}$ = value of trace element (grams per ton of rock); and
d_v = density of the sample (grams per cubic centimeter).

We used equation 3 in our recalculations of data on contents of trace elements.

RESULTS AND DISCUSSION

Basalt Petrography and Geochemistry

The basalts from the Kerguelen Plateau are represented by aphyric and sparsely porphyritic varieties (Coffin, Frey, Wallace, et al., 2000). Tables T3, T4, T5, and T6 summarize the petrographic compositions of the samples studied. Aphyric basalts dominate in most Leg 183 holes. Rarer porphyritic basalts prevail in Holes 1140A and 1137A. Phenocrysts are represented mainly by plagioclase. Phenocrysts of olivine and clinopyroxene are rare (Hole 1137A). The total quantity of phenocrysts within porphyritic basalts varies from single crystals through 25% of the rock volume. Both the degree of crystallinity and vesicularity of the basalts vary greatly. Massive basalts are rare but most common in the northern part of the Kerguelen Plateau (Hole 1140A). Less vesicular basalts are recognized in Holes 1136A and 1138A. Both intergranular and intersertal textures are dominant. Vitrophyric texture is present occasionally (Hole 1140A).

The results of chemical analyses of the basalts from Holes 1136A, 1137A, 1138A, and 1140A (Leg 183) and from Hole 747C (Leg 120) are given in Table T7. To plot petrochemical diagrams, we have recalculated concentrations of major elements to the dry residue (recalculated to 100%). In plotting diagrams, we did not use the following samples: Z-1012 (Sample 183-1137A-34R-3, 18–23 cm), Z-1014 (Sample 39R-2, 114–119 cm), Z-1016 (Sample 43R-2, 84–92 cm), Z-1017 (Sample 45R-1, 121–126 cm), and Z-1018 (Sample 78R-1, 60–64 cm), as they represent litho- and crystalloclastic dacitic tuffs, tuff/basalt contact, and highly altered basalt.

On the (Na_2O + K_2O)-SiO_2 diagram, basalts from the Kerguelen Plateau plot in both tholeiitic and alkaline fields (Fig. F1). Holes 1140A, 749C, and 750B provide exceptions, as they contain only tholeiitic basalts.

On the three-component diagram, Zr-Nb-Y (Fig. F2), the data plot in a compact field in the area of normal mid-ocean-ridge basalt (N-MORB) (Holes 1136A and 1140A), in the area of intraplate tholeiites (Holes 1137A, 1138A, and two samples from Hole 1140A), and the basalts from Hole 747C plot in two fields enriched by MORB (basalts from plume-influenced regions [P type]) and intraplate oceanic tholeiites.

In most cases, basalts from each hole (except Hole 1140A) demonstrate similar REEs in both concentration and distribution patterns, indicative of a common mantle source (Fig. F3). REE distribution indicates that basalts from Holes 1136A, 1137A, 1138A, and 747C are enriched in light rare earth elements (LREEs) in comparison with normal tholeiitic basalts of mid-ocean ridges.

The variational REE diagram for basalts from Hole 1140A (Fig. F3) seems to show two groups. The trend for low-Ti basalts (group 1) is similar to that typical for normal oceanic tholeiites. The trend for high-Ti basalts (group 2) is enriched in LREEs. This suggests that melts, which formed the basalts recovered from Hole 1140A, belong to two sources from different depths.

Figure F4 demonstrates average REE distribution in basalts from holes drilled on the Kerguelen Plateau. Judging from both the REE values and the distribution pattern, basalts from Hole 750B in the southern part of the Kerguelen Plateau are similar to N-MORB. This provides evidence that their initial melts derived from depleted mantle sources.

T3. Petrographic descriptions of analyzed basalts and XRD of secondary minerals, Hole 1136A, p. 21.

T4. Petrographic descriptions of analyzed basalts and XRD of secondary minerals, Hole 1137A, p. 22.

T5. Petrographic descriptions of analyzed basalts and XRD of secondary minerals, Hole 1138A, p. 24.

T6. Petrographic descriptions of analyzed basalts and XRD of secondary minerals, Hole 1140A, p. 26.

T7. Basalts, Holes 1136A, 1137A, 1138A, 1140A, and 747C, p. 28.

F1. (Na_2O + K_2O)-SiO_2 diagram, p. 13.

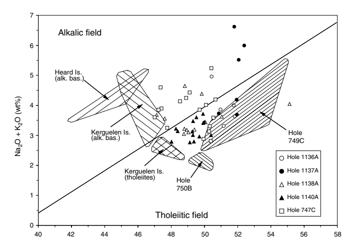

F2. Discrimination Nb-Zr-Y diagram for basalts, Holes 1136A, 1137A, 1138A, 1140A, and 747C, p. 14.

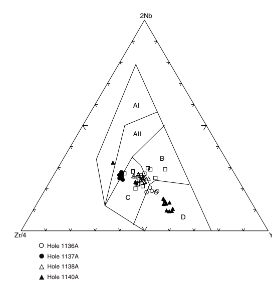

The same is also evident in group 1 basalts from Hole 1140A. Basalts from Holes 1136A and 749C are similar in REE values and distribution of average composition of enriched mid-ocean-ridge basalts (E-MORBs). Basalts from Holes 1138A and 1140A (group 2), and especially those from the Elan Bank (Hole 1137A), are derived from significantly enriched (compared to N-MORB) sources. The basalts from Hole 747C (central part of the Kerguelen Plateau) and tholeiites from Kerguelen Island are similar in REE values and distribution. They demonstrate both LREE and LREE/heavy rare earth elements (HREE) values higher than E-MORB. Alkaline basalts from the Kerguelen and Heard Islands demonstrate the highest values of these parameters.

Alteration

Hole 1136A

Thin sections show that the basalts from Hole 1136A are weakly to moderately altered (Table T3). According to whole-rock chemical analyses, altered basalts contain 0.90–1.58 wt% H_2O^+ (Table T7). The degree of rock oxidation is moderate. Both olivine and interstitial glass are completely replaced by smectite-chlorite aggregate. Plagioclase is partly replaced by smectite-chlorite aggregate. Vesicles are filled mainly with smectite (Table T8). Veins are filled with calcite. Secondary minerals identified in basalts from Hole 1136A, from vesicles and veins (Table T8) and from groundmass (Table T3), indicate a low-temperature environment for water-rock interaction.

Hole 1137A

Thin section examination indicated that basalts from Hole 1137A are more altered than those from Hole 1136A. We estimate the degree of basalt alteration as 10%–60% (Table T4). Chemical analyses show that the altered basalts contain 0.19–3.03 wt% H_2O^+ (Table T7). The Fe_2O_3/FeO ratio varies from 0.88 to 3.57 (Table T7) and also indicates various degrees of basalt oxidation. Tuff (Sample 183-1137A-43R-2, 84–92 cm) is strongly altered (80%; estimate based on the thin section analysis) (Table T4) and highly oxidized (Fe_2O_3/FeO = 10.14) (Table T7).

Thin sections show that ferromagnesian minerals in phenocrysts, groundmass, and intersertal glass are completely replaced by chlorite and chlorite-smectite aggregates. Plagioclase phenocrysts in porphyritic basalt (Sample 183-1137A-45R-1, 121–126 cm) are replaced with K-feldspar (adularia?), smectite-chlorite aggregates, and carbonate (Table T4). Plagioclase from the matrix also is replaced with K-feldspar. The degree of alteration is high (40%) (Table T4). Highly altered tuff (Sample 183-1137A-43R-2, 84–92 cm) contains pseudomorphs of chlorite and carbonate derived from alteration of a prismatic minerals. Biotite is chloritized. Interstitial glass is replaced by smectite-chlorite aggregate.

In basement Subunit 2A and Unit 4 (Hole 1137A), smectite is the most common mineral filling vesicles (Table T9). Often, it is present with some admixture of clinoptilolite and heulandite. An admixture of a 7-Å mineral (probably dickite) and calcite is also present. In Subunits 7A and 8A, vesicles also contain chlorite phases (Table T9). Subunit 7A (Sample 183-1137A-37R-5, 73–79 cm) contains a mixed-layer smectite-chlorite mineral. Chlorite, a dominant mineral, is present below (Sample 183-1137A-39R-3, 6–14 cm) and is also accompanied by defective chlorite (Sample 39R-2, 114–119 cm). Defective chlorite was identified

F3. N-MORB normalized rare earth element abundances in basalts, Holes 1136A, 1137A, 1138A, 1140A, and 747C, p. 15.

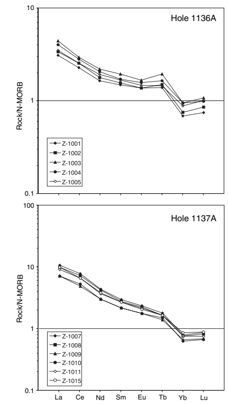

F4. Chondrite-normalized rare earth element abundances in average basalts, Holes 1136A, 1137A, 1138A, 1140A, and 747C, p. 18.

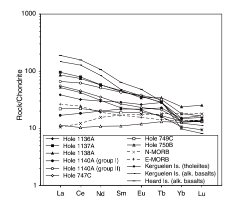

T8. Secondary minerals, Hole 1136A, p. 32.

T9. Secondary minerals, Hole 1137A, p. 33.

according to Drits and Tchoubar (1990). Clinoptilolite, hydromica, and quartz are also present with smectite and chlorite.

We studied two veins in the basalt section of Hole 1137A (Table T9). Veinlets contain smectite, calcite, and clinoptilolite and quartz in trace amounts.

The alteration zone between the basalt and tuff (green matter; Sample 183-1137A-34R-3, 18–23 cm) contains mixed-layer hydromica-smectite minerals and hydromica and quartz in trace amounts (Table T9). The appearance of hydromica phases probably indicates water migration in an oxidizing environment.

The entire complex of secondary minerals in basalts from Hole 1137A (Tables T4, T9) indicates the low-temperature conditions of alteration and shows absence of vertical zonation in secondary minerals in the basalt section in total. The presence of dickite in trace amounts in the upper part of Subunit 2A and Unit 4 provides evidence of subaerial weathering.

Hole 1138A

Examination of the basalt section from Hole 1138A shows that alteration varies from slight to intense (from 10% to 50%) (Table T5). By chemical analysis, they contain 0.36–4.96 wt% H_2O^+ (Table T7). The basalts are mostly nonoxidized or only slightly oxidized as suggested by dark gray color, study of thin sections, and Fe_2O_3/FeO ratio. The latter varies from 0.40 to 2.06 (Table T7). In contrast, tuff (Sample 183-1138A-78R-1, 60–64 cm) is strongly oxidized, with an Fe_2O_3/FeO ratio of 25.64 and altered (60% in thin section) (Table T5).

Olivine is completely replaced by pale green chlorite. Plagioclase is partly replaced by chlorite. The interior of the plagioclase is replaced by a micaceous mineral (Sample 183-1138A-84R-5, 20–25 cm). Interstitial glass is completely replaced by chlorite and smectite-chlorite aggregates (Table T5).

Secondary minerals filling vesicles in basalt from Hole 1138A (Tables T10, T11) are characteristic and distinct from those of other Leg 183 holes in the abundance of zeolites (heulandite, clinoptilolite, mordenite, stilbite, analcime, and natrolite). Thomsonite is present occasionally. No vertical zonation of zeolite distribution in Hole 1138A is obvious. For example, clinoptilolite and heulandite are present in basalts in various parts of the basalt section recovered from Hole 1138A. Mordenite is present only in basalt from Unit 6 (Sample 183-1138A-81R-1, 34–39 cm, 30 cm below the top of the lava flow). Analcime and stilbite are present in vesicles and veins of basalts from Units 17 and 19. These minerals are absent from other parts of the basalt section. Clay minerals also lack any vertical zonation (Tables T5, T10). All secondary minerals (clay and nonclay minerals) studied in vesicles and veins, as well as in basalt groundmass, show no vertical zonation in their distribution throughout the basalt section in Hole 1138A.

T10. Secondary minerals, Hole 1138A, p. 34.

T11. Microprobe analyses of clay minerals and zeolites, Hole 1138A, p. 35.

The abundance of zeolites in basalts from Hole 1138A (in comparison with other Leg 183 holes) is probably related to its closer location to the paleoeruptive center. The presence of several varieties of zeolites and great variation in chemical composition is characteristic of rock alteration in hydrothermal systems.

Within individual lava flows, there are no limitations on the presence of smectite. It fills vesicles near the top of basalt flows, for example, at 4, 20, and 30 cm below the top of the lava flows (Samples 183-1138A-88R-2, 91–96 cm; 82R-2, 76–81 cm; and 81R-1, 34–39 cm, respectively), at the bottom of Unit 17 (Sample 86R-3, 72–74 cm), or at 90 cm above the bottom of Unit 10 (Sample 83R-4, 19–24 cm) (Table T10). Besides marginal parts of lava flows, smectite is present in the interior of basalt Units 6, 9, 11, 13, and 19 (Samples 183-1138A-81R-2, 51–57 cm; 82R-5, 19–23 cm; 83R-5, 106–109 cm; 84R-5, 20–25 cm; and 87R-2, 76–81 cm). All determinations of chlorite, defective chlorite, and serpentine(?) were made from interior and basal parts of basalt flows (Table T10).

The absence of any vertical zonation in secondary minerals in basalt sections in total and the presence of zonation within individual flows had been shown in basalts from Suiko Guyot in the Emperor Seamount Chain (Hole 433C, Leg 55) (Kurnosov, 1986), most impressively in Unit 48 (7.5 m thick). Smectite dominates at the top and bottom of the flow, whereas toward centre of the flow, smectite replaced swelling chlorite. Mixed-layer chlorite-swelling chlorite dominates in the flow interior. A similar distribution of secondary minerals and lack of vertical zonation were recognized in the West Pacific Guyots, Hole 865A, Legs 143 and 144 (Kurnosov et al., 1995). Basalt flows in Allison Guyot suffered low-temperature smectitization, mainly in the upper parts of the units, and chloritization (swelling chlorite and mixed-layer smectite-chlorite mineral) in the interior.

The secondary minerals have probably formed under the influence of individual basalt flows in an environment dominated by horizontal migration of water, primarily along contacts between lava flows. The influence of hot waters of interlayer-fissure circulation on the formation of subhorizontal zeolite zones in basalts is well known in Iceland (Walker, 1960; Tomasson and Kristsmannsdottir, 1972; Kristsmannsdottir and Tomasson, 1978).

Hole 747C

Hole 747C is located near Hole 1138A. The basalts studied from Hole 747C show various degrees of alteration (H_2O^+ varies from 0.69 to 5.14 wt%) (Table T7). In altered basalts, dominant secondary minerals are represented by smectite, or smectites with chlorite or swelling chlorite, and chlorite. Zeolites were determined in amygdules, in the groundmass, and in altered plagioclase phenocrysts. Zeolites are represented by chabazite, natrolite, thomsonite, mesolite, stilbite, and heulandite (Sevigny et al., 1992). Comparison of zeolite and clay minerals in Leg 183 and 120 basalts and in Iceland (Kristmannsdottir and Tomasson, 1978) suggests that alteration of basalts from the central part of the Kerguelen Plateau (Holes 1138A and 747C) occurred at a temperature of 120°C.

Two types of alteration, oxidative and nonoxidative, are recognized in Hole 747C. Oxidative zones are marked by goethite, Fe hydroxides, calcite, and celadonite(?). This secondary mineral assemblage forms at sites of low-temperature water-basalt interaction (Bass, 1976; Bass et al., 1973; Kurnosov, 1986).

Hole 1140A

Basalts from pillow lavas of Hole 1140A are less altered than basalts from other Leg 183 holes. Thin sections indicate alteration of basalts of 5% to 20% (Table T6). Only two samples had alteration of a moderate to high degree, from 25% to 35%. The basalts are fresh or scarcely oxidized. The Fe_2O_3/FeO ratio is low and varies from 0.53 to 1.07 (Table T7). In only two samples, the ratio was 2.41 and 2.31.

Aggregates of chlorite-smectite replace olivine. Plagioclase is completely replaced with chlorite-smectite aggregate or with a mica-type mineral. Interstitial glass is completely replaced by chlorite or chlorite and ore minerals (Table T6). Smectites dominate in the fine fraction that was removed from the basalts (Table T6).

In four samples, vesicles are filled with smectite; the vein sampled from the glass is filled with calcite (Table T12). Joint fissures are covered, in one case, with a thin layer of smectite and defective chlorite and, in the other case, smectite with traces of serpentine(?) and quartz.

T12. Secondary minerals, Hole 1140A, p. 36.

Zeolites have not been identified, and this is the principal difference in basalt alteration from Hole 1140A (submarine extrusion) compared with those from Holes 1136A, 1137A, and, especially, Hole 1138A (subaerial extrusion).

Thus, pillow lava basalts from Hole 1140A have a low degree of alteration and most are not oxidized. Secondary minerals indicate a low-temperature alteration environment. Circulation of hotter fluids probably occurred along cracks now filled with smectite, defective chlorite, serpentine(?), and quartz. Nevertheless, these probable fluids did not play a significant role in the alteration of the basalt section of Hole 1140A.

Estimation of Chemical Element Gain/Loss

We studied mobility of chemical elements in relation to alteration of basalts under both oxidative and nonoxidative environments (Bass 1976; Bass et al., 1973). To estimate chemical element mobility, we used data on the amount of major and minor elements (grams per 1000 cm^3) in basalts (Table T13).

T13. Abundance of major and trace elements, Holes 1136A, 1137A, 1138A, and 1140A, p. 37.

Table T14 shows two examples of mass balance from nonoxidative and oxidative environments of alteration of basalts from the Kerguelen Plateau.

T14. Mass balance at low-temperature alteration of the basalts from the Kerguelen Plateau, p. 40.

Basalts from Hole 1140A have similar degrees of alteration. Nevertheless, they are favorable for analyzing the mobility of chemical element in a "pure" nonoxidized environment, as they are neither oxidized nor vesicular. For further reference, we chose Sample 183-1140A-35R-1, 35–42 cm, where H_2O^+ = 0.74 wt%; Fe_2O_3/FeO ratio = 1.01; and density = 2.93 g/cm^3 (Tables T7, T14). For comparison we chose nonoxidized Sample 183-1140A-34R-1, 117–121 cm, where H_2O^+ = 1.40 wt%; Fe_2O_3/FeO ratio = 0.69; and density = 2.57 g/cm^3. The trend to a decrease under nonoxidative alteration in basalt is most evident in major elements, REEs, Cu, Nb, Zr, Y, Rb, and Sr (Table T14). Ni, V, Co, Zn, and Ba show a weak trend to increase during alteration.

Sample 183-1137A-27R-1, 100–105 cm (Fe_2O_3/FeO = 3.57 and H_2O^+ = 2.03 wt%), is oxidized (Table T7) and highly vesicular (Table T14). Hence, for comparison, we chose relatively fresh nonoxidized basalt with similar vesicularity (Sample 183-1137A-39R-2, 114–119 cm; H_2O^+ = 0.99 wt%). Comparison revealed that oxidizing alteration leads mostly to the accumulation of Fe, Mg, Ca, P, REEs, Co, Zr, and Ba in basalts (Table T14). This is especially evident for Sr. In contrast, Si, Al, Mn, Na, K, Ni, V, Cu, Y, and Rb show a decrease.

This study has shown that the mobility of chemical elements during alteration of basalts from the Kerguelen Plateau is different in oxidizing and nonoxidizing environments. We conclude that generally in nonoxidizing alteration environments, basalts lose most elements. In contrast, in oxidizing alteration, basalts accumulate many elements. The degree of alteration of basalts (selected for estimation of chemical element mobility) is low, so the mobility of elements seems to be at the rudimentary stage.

ACKNOWLEDGMENTS

The research used samples and data provided by the Ocean Drilling Program (ODP). ODP is sponsored by the U.S. National Science Foundation (NSF) and participating countries under management of Joint Oceanographic Institutions (JOI), Inc. Funding for this research was provided by the Russian Foundation for Fundamental Research (numbers 98-05-64856 and 99-05-65462).

We thank the reviewers for useful critical remarks. We also would like to thank S.M. Liapunov (XRF and neutron-activation analysis), I.Y. Lubchenko (atomic emission spectroscopy), and N. Kalashnikova and G. Granovsky (wet chemical analysis).

REFERENCES

Bass, M.N., 1976. Secondary minerals in oceanic basalt, with special reference to Leg 34, Deep Sea Drilling Project. *In* Yeats, R.S., Hart, S.R., et al., *Init. Repts. DSDP,* 34: Washington (U.S. Govt. Printing Office), 393–432.

Bass, M.N., Moberly, R., Rhodes, J.M., Shih, C.C., and Church, S.E., 1973. Volcanic rocks cored in the central Pacific, Leg 17, Deep Sea Drilling Project. *In* Winterer, E.L., Ewing, J.I., et al., *Init. Repts. DSDP,* 17: Washington (U.S. Govt. Printing Office), 429–503.

Coffin, M.F., Frey, F.A., Wallace, P.J., et al., 2000. *Proc. ODP, Init. Repts.,* 183 [CD-ROM]. Available from: Ocean Drilling Program, Texas A&M University, College Station, TX 77845-9547, USA.

Drits, V.A., and Tchoubar, C., 1990. *X-Ray Diffraction by Disordered Lamellar Structures (Theory and Applications to Microdivided Silicates and Carbons):* Heidelberg (Springer-Verlag).

Gladney, E.S., and Roelandts, I., 1988. 1987 compilation of elemental concentration data from USGS BHVO-1, MAG-1, QLO-1, RGM-1, SCo-1, SDC-1, SGR-1 and STM-1. *Geostand. Newsl.,* 12:253–262.

Kazitzyn, Y. and Rudnik, V., 1968. *Guide to Estimation of Mass Balance and Inner Energy during Metasomatic Rocks Formation:* Moscow (Nedra).

Kristmannsdóttir, H., and Tómasson, J., 1978. Zeolite zones in geothermal areas in Iceland. *In* Sand, L.B., and Mumpton, F.A. (Eds.), *Natural Zeolites: Occurrences, Properties, and Use:* Oxford (Pergamon), 277–284.

Kurnosov, V.B., 1986. *Hydrothermal Alterations of Basalts in the Pacific Ocean and Metal-bearing Deposits, Using Data of Deep-sea Drilling:* Moscow (Nauka).

Kurnosov, V.B., and Murdmaa, I.O., 1996. Hydrothermal and cold-water circulation within the intraplate seamounts: effects on rock alteration. In *The Oceanic Lithosphere and Scientific Drilling into the 21st Century:* Durham, United Kingdom (InterRidge Office, Univ. Durham), 87–88. (Abstract)

Kurnosov, V., Zolotarev, B., Eroshchev-Shak, V., Artamonov, A., Kashinzev, G., and Murdmaa, I., 1995. Alteration of basalts from the West Pacific Guyots, Legs 143 and 144. *In* Haggerty, J.A., Premoli Silva, I., Rack, F., and McNutt, M.K. (Eds.), *Proc. ODP, Sci. Results,* 144: College Station, TX (Ocean Drilling Program), 475–491.

Macdonald, G.A., 1968. Composition and origin of Hawaiian lavas. *Contrib. Hawaii Inst. Geophys. Year.,* 477–552.

Meschede, M., 1986. A method of discriminating between different types of mid-oceanic ridge basalts and continental tholeiites with the Nb-Zr-Y diagram. *Chem. Geol.,* 56:207–218.

Salters, V.J.M., Storey, M., Sevigny, J.H., and Whitechurch, H., 1992. Trace element and isotopic characteristics of Kerguelen-Heard Plateau basalts. *In* Wise, S.W., Jr., Schlich, R., et al., *Proc. ODP, Sci. Results,* 120: College Station, TX (Ocean Drilling Program), 55–62.

Sevigny, J.H., Whitechurch, H., Storey, M., and Salters, V.J.M., 1992. Zeolite-facies metamorphism of central Kerguelen Plateau basalts. *In* Wise, S.W., Jr., Schlich, R., et al., *Proc. ODP, Sci. Results,* 120: College Station, TX (Ocean Drilling Program), 63–69.

Storey, M., Kent, R.W., Saunders, A.D., Salters, V.J., Hergt, J., Whitechurch, H., Sevigny, J.H., Thirlwall, M.F., Leat, P., Ghose, N.C., and Gifford, M., 1992. Lower Cretaceous volcanic rocks on continental margins and their relationship to the Kerguelen Plateau. *In* Wise, S.W., Jr., Schlich, R., et al., *Proc. ODP, Sci. Results,* 120: College Station, TX (Ocean Drilling Program), 33–53.

Storey, M., Saunders, A.D., Tarney, J., Leat, P., Thirlwall, M.F., Thompson, R.N., Menzies, M.A., and Marriner, G.F., 1988. Geochemical evidence for plume-mantle interactions beneath Kerguelen and Heard Islands, Indian Ocean. *Nature,* 336:371–374.

Sun, S.-S., and McDonough, W.F., 1989. Chemical and isotopic systematics of oceanic basalts: implications for mantle composition and processes. *In* Saunders, A.D., and Norry, M.J. (Eds.), *Magmatism in the Ocean Basins*. Spec. Publ.—Geol. Soc. London, 42:313–345.

Tomasson, J., and Kristmannsdottir, H., 1972. High temperature alteration minerals and geothermal brine, Reykjanes, Iceland. *Contr. Mineral. Petrol.,* 36:123–134.

Vallier, T.L., Rea, D.K., Dean, W.E., Thiede, J., and Adelseck, Ch.G., 1981. The geology of Hess Rise, Central North Pacific Ocean. *In* Thiede, J., Vallier, T.L., et al., *Init. Repts. DSDP,* 62: Washington (U.S. Govt. Printing Office), 1031–1072.

Walker, G.P.L., 1960. Zeolite zones and dike distribution in relation to the structure of the basalts in eastern Iceland. *J. Geol.,* 68:515–528.

Figure F1. ($Na_2O + K_2O$)-SiO_2 diagram (Macdonald, 1968) for basalts from the Kerguelen Plateau. Fields for Kerguelen and Heard Islands basalts are from Storey et al. (1988); Kerguelen Plateau (Holes 749C and 750B) data are from Storey et al. (1992). Is. = island. alk. bas. = alkalic basalt.

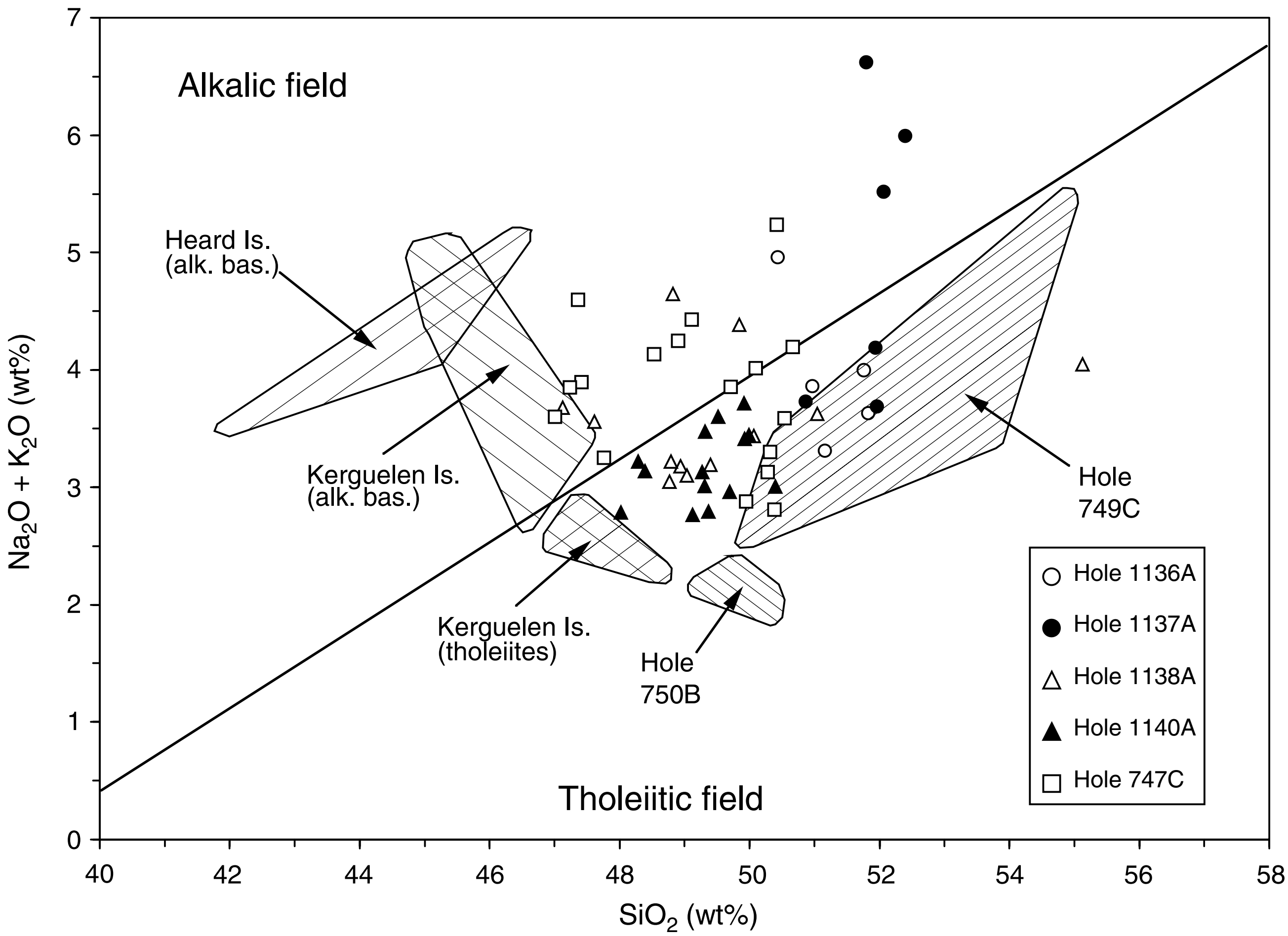

Figure F2. Discrimination Nb-Zr-Y diagram (Meschede, 1986) for basalts from Holes 1136A, 1137A, 1138A, and 1140A (Leg 183) and Hole 747C (Leg 120). AI, AII = fields of intraplate alkali basalts; AII, C = fields of intraplate tholeiites; B = field of P-type MORB; D = field of N-type MORB; C, D = fields of volcanic arc basalts.

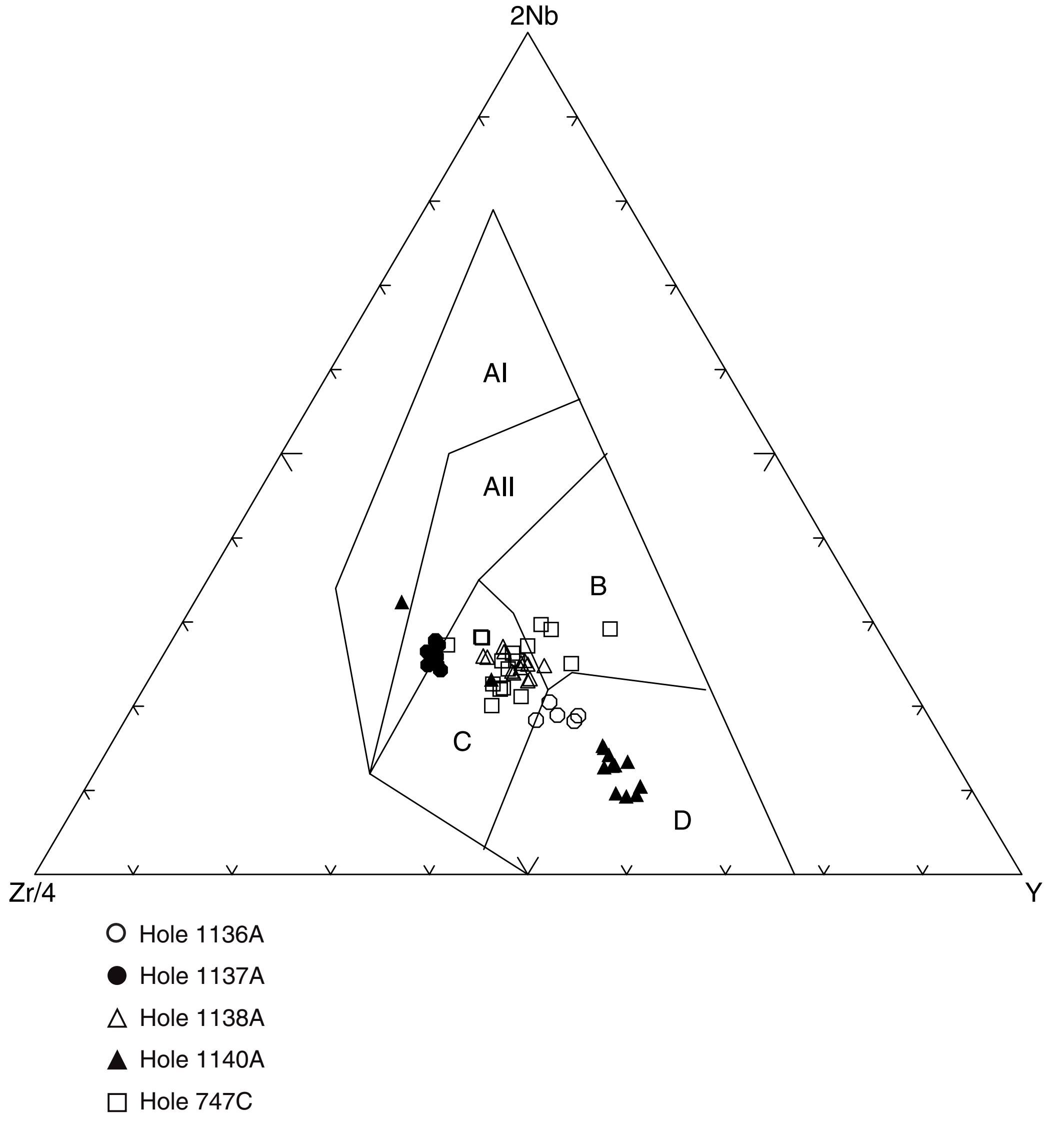

Figure F3. Normal mid-ocean-ridge basalt (N-MORB)-normalized rare earth element abundances in basalts from Holes 1136A, 1137A, 1138A, and 1140A (Leg 183) and Hole 747C (Leg 120). Normalizing values are from Sun and McDonough (1989). (Continued on next two pages.)

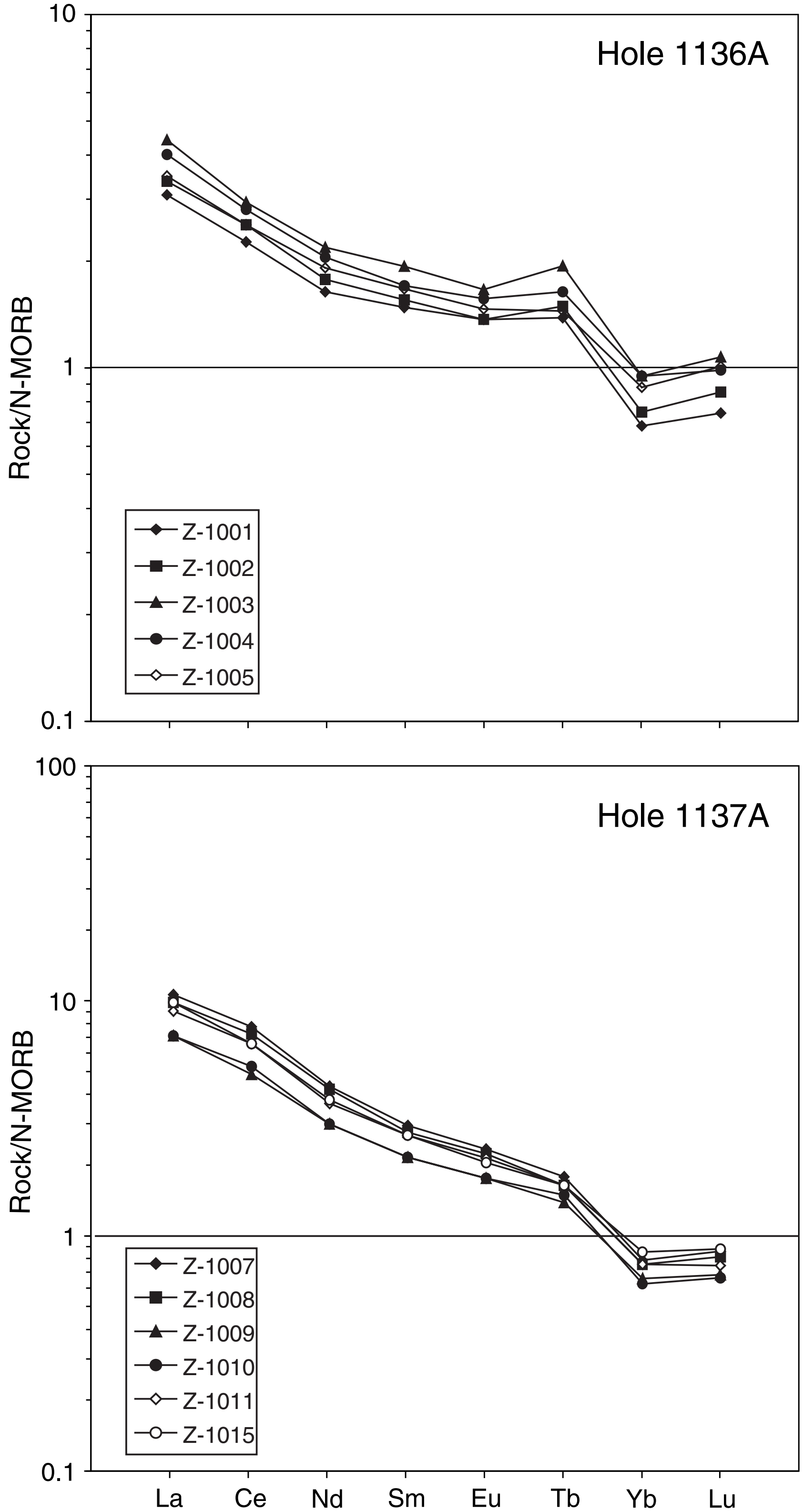

Figure F3 (continued).

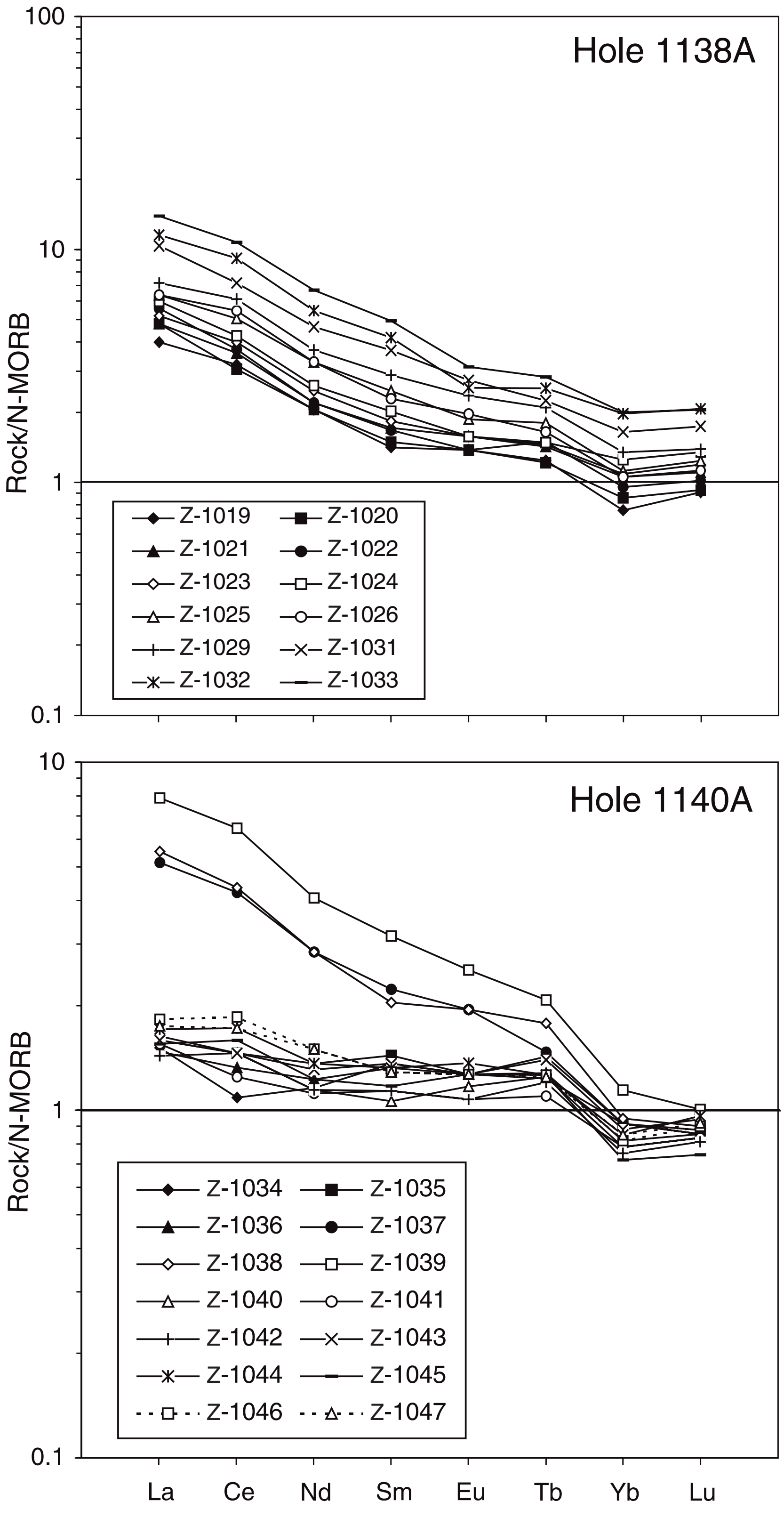

Figure F3 (continued).

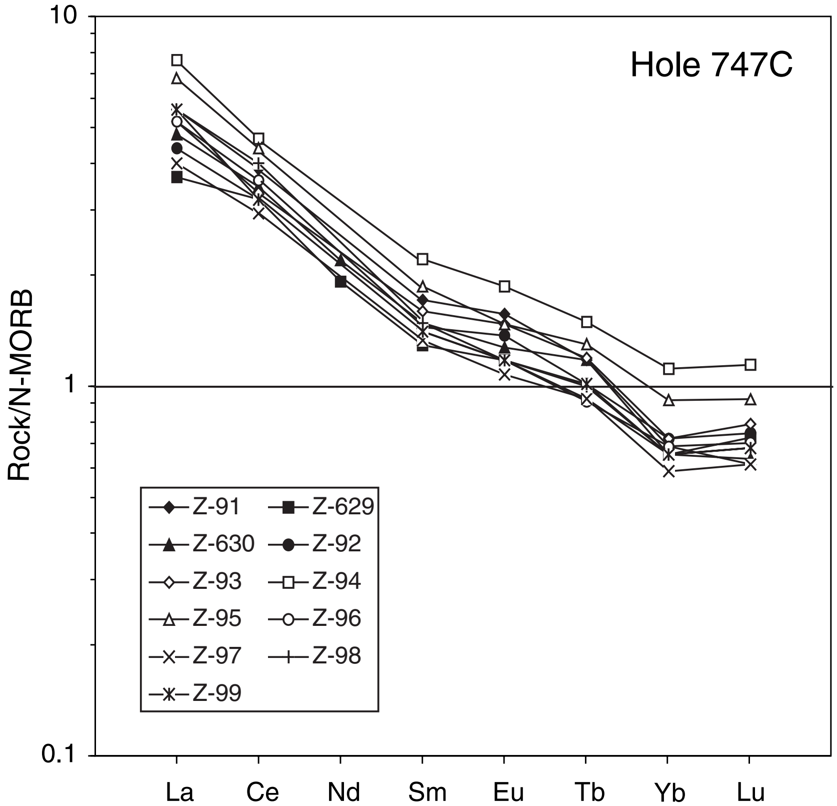

Figure F4. Chondrite-normalized rare earth element abundances in average basalts from Holes 1136A, 1137A, 1138A, and 1140A (Leg 183) and Hole 747C (Leg 120); Kerguelen and Heard Islands (Storey et al., 1988); Holes 749C and 750B (Leg 120) (Storey et al., 1992; Salters et al., 1992). Normalizing normal mid-ocean-ridge basalt (N-MORB) and enriched mid-ocean-ridge basalt (E-MORB) values are from Sun and McDonough (1989). Is. = island. alk. = alkaline.

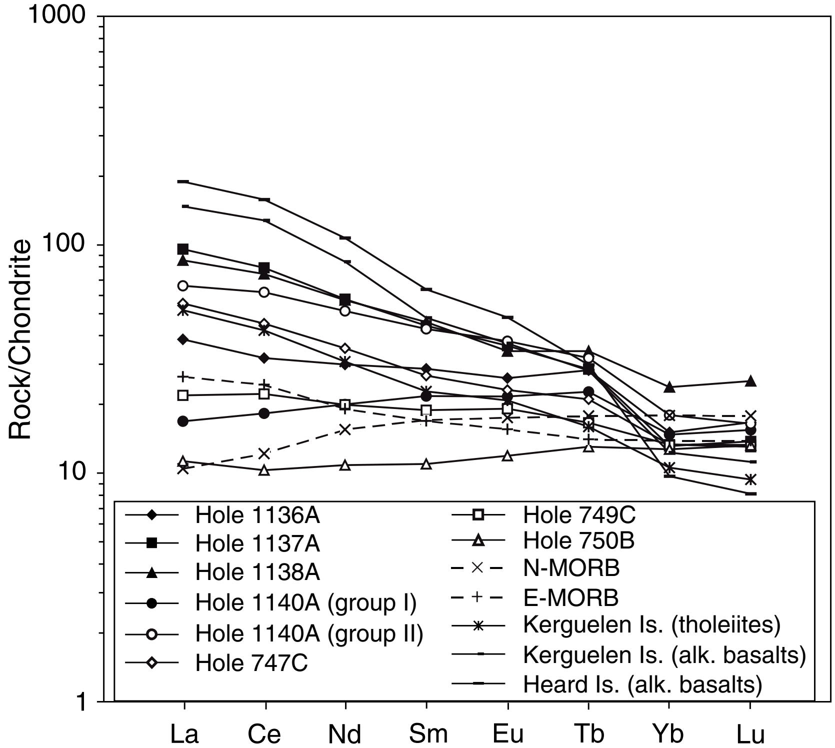

Table T1. Values of the transitional coefficient R_o.

Oxide	R_o (wt%)
SiO_2	1.002
TiO_2	0.754
Al_2O_3	1.182
Fe_2O_3	0.754
FeO	0.838
MnO	0.849
MgO	1.494
CaO	1.074
Na_2O	1.944
K_2O	1.279
P_2O_5	0.849
H_2O	6.688
CO_2	1.369

Notes: Kazitzyn and Rudnik, 1968. R_o = transitional coefficient.

Table T2. Values of coefficient K.

Oxide	K (wt%)
SiO_2	4.672
TiO_2	5.995
Al_2O_3	5.294
Fe_2O_3	6.990
FeO	7.769
MnO	7.743
MgO	6.030
CaO	7.146
Na_2O	7.419
K_2O	8.302
P_2O_5	4.365
H_2O	1.119
CO_2	2.730

Note: $K = 0.166 \times a_i \times R_o$.

Table T3. Brief petrographic descriptions of analyzed basalts and X-ray diffraction of secondary minerals from fine fraction removed from altered volcanic rocks, Hole 1136A.

Core, section, interval (cm)	Description	Alteration	XRD identification
183-1136A-			
15R-2, 30–36	Olivine-plagioclase glomerophyric basalt, vesicular (15%), incompletely crystallized, with intersertal texture. Phenocrysts (10%–15%) are tabular crystals of plagioclase (labradorite) with size 0.3–1.2 mm and single grains of olivine. Groundmass is plagioclase lathe, clinopyroxene, opaque minerals, and interstitial glass (10%–15%).	Moderate (~25%–30%); vesicles infilled with smectite and chlorite. Phenocrysts of olivine completely replaced by smectite and chlorite. Oxidation of basalt is low (~5%).	Smectite and hydromica in trace amounts
16R-1, 113–118	Sparsely plagioclase phyric basalt, vesicular (~8%). Groundmass demonstrates intergranular texture. Phenocrysts represented by tabular crystals of plagioclase (0.4- to 3-mm labradorite compose up to 5% of rock) and single grains of olivine. Groundmass is plagioclase lathe, clinopyroxene, single grains of olivine, opaque minerals and dust, and interstitial glass (5%–7%).	~15%–20%; vesicles infilled with smectite and chlorite. Phenocrysts of olivine and interstitial glass completely replaced by smectite and chlorite. Oxidation of basalt is low (~3%–5%).	Smectite
17R-2, 84–90	Sparsely plagioclase phyric basalt, weakly vesicular (~5%; 0.08–0.15 mm), incompletely crystallized, with intergranular texture. Phenocrysts of tabular crystals of plagioclase (up to 1 mm) labradorite (~5% of rock). Groundmass is plagioclase lathe (45%–50%), clinopyroxene (30%–35%), opaque minerals (5%), and interstitial glass (10%).	~15%; interstitial glass completely replaced by smectite and chlorite. Rock is nonoxidized.	Smectite
18R-2, 62–67	Plagioclase phyric basalt, vesicular (~10%), incompletely crystallized, with intersertal texture. Phenocrysts of tabular crystals of plagioclase (0.3–2.5 mm) labradorite (5%–10% of rock). Groundmass is plagioclase lathe (45%–50%), microlathe of clinopyroxene (30%–35%), opaque minerals (2%–3%), and interstitial glass (10%–15%).	~15%–20%; vesicles infilled with smectite and chlorite; interstitial glass completely and partially replaced with smectite and chlorite. Rock is nonoxidized.	Smectite
19R-1, 27–31	Plagioclase phyric basalt, vesicular (~10%), incompletely crystallized, with interstitial texture. Sample is same as Sample 183-1136A-18R-2, 62–67 cm.	~10%–15%. Rock is nonoxidized.	Smectite

Note: XRD = X-ray diffraction.

Table T4. Brief petrographic descriptions of analyzed basalts and X-ray diffraction of secondary minerals from fine fraction removed from altered volcanic rocks, Hole 1137A. (**See table note.** Continued on next page.)

Core, section, interval (cm)	Description	Alteration	XRD identification
183-1137A-			
25R-4, 100–115	Aphyric basalt, vesicular (20%–25%; 0.1–0.5 mm), incompletely crystallized. Groundmass with microdoleritic texture. Phenocrysts of long lathe of plagioclase (andesine; 0.1–0.3 mm). Dark brown volcanic glass with opaque dust and clinopyroxene.	Moderate (30%–35%); vesicles completely or partly infilled by clay minerals, zeolites, and carbonate. Oxidation of basalt is ~30%.	
27R-1, 100–105	Sparsely plagioclase microphyric basalt, vesicular (5%–10%; up to 2–4 mm), incompletely crystallized. Groundmass of vitrophyric-microlitic texture. Phenocrysts of crystals of plagioclase (<1%; 0.5–0.6 mm).	~25%–30%; clinopyroxene completely replaced by chlorite; plagioclase is partly replaced with chlorite; vesicles infilled zonally (from walls to center of vesicles) with smectite, zeolite, and trace of chlorite, carbonate is located in center. Oxidation of basalt is low (~5%).	Smectite
29R-1, 38–43	Sparsely olivine-plagioclase microphyric basalt, weakly vesicular (1%; 0.1–0.3 mm), incompletely crystallized. Groundmass of intergranular, partly microdoleritic, texture. Microphenocrysts of single tabular crystals of plagioclase (andesine; to 0.2–0.4 mm) and olivine. Groundmass of plagioclase lathe (50%), isometric clinopyroxene crystals (30%–35%), opaque minerals, and interstitial glass (5%–10%).	~20%; olivine and interstitial glass completely replaced by smectite and chlorite; vesicles infilled with smectite and chlorite. Oxidation of basalt is low (~5%).	Smectite
29R-3, 5–9	Olivine-clinopyroxene-plagioclase phyric basalt, vesicular (10%–15%; 1–2 to 5 mm), incompletely crystallized. Groundmass with vitrophyric-microlitic texture. Phenocrysts (5%–10%) of olivine (0.2–0.7 mm), clinopyroxene (0.2–1 mm), and plagioclase (up to 1.3–1.5 mm). Groundmass of plagioclase lathe (50%), clinopyroxene, and dark brown interstitial glass.	~15%–20%; olivine and interstitial glass completely replaced by smectite and chlorite; vesicles infilled with smectite and chlorite, with admixture of zeolites and carbonate. Oxidation of basalt is low (~5%).	
32R-3, 71–76	Clinopyroxene-plagioclase glomerophyric basalt, massive. Phenocrysts of clinopyroxene (0.2–0.5 mm) and plagioclase (labradorite and andesine) (to 0.3–1.2 mm). Groundmass of plagioclase lathe (45%–50%), clinopyroxene (30%–35%), opaque minerals (5%), and interstitial glass (10%).	10%–15%; olivine replaced by smectite, chlorite, and oxidized Fe, interstitial glass replaced by smectite and chlorite. Oxidation of basalt is low (~2%).	Smectite and defective chlorite in trace amounts
32R-7, 46–50	The sample is similar to Sample 183-1137A-32R-3, 71–76 cm.	10%–15%; olivine completely replaced by smectite, chlorite, and oxidized Fe, interstitial glass replaced by smectite and chlorite. Oxidation of basalt is low (~2%).	Smectite
34R-3, 18–23	Contact of tuff and basalt:		
	1. Sparsely plagioclase microphyric basalt, weakly vesicular (single vesicles), incompletely crystallized. Groundmass demonstrates microlitic texture. Microphenocrysts of plagioclase (<5%; to 0.1–0.55 mm). Groundmass represented by glass and long lathe of plagioclase.	Moderate (~30%); microphenocrysts replaced completely by opaque minerals and traces of chlorite; interstitial glass replaced by chlorite and smectite and opaque minerals. Groundmass plagioclase replaced by albite; single vesicles infilled with opaque minerals and chlorite. Oxidation of basalt is moderate (~10%).	Smectite and hydromica, chlorite, and swelling chlorite in trace amounts
	2. Crystal-lithoclastic tuff, vesicular.	Moderate (~30%). Oxidation of basalt is moderate (~10%).	Smectite and hydromica and quartz in trace amounts
37R-5, 73–79	Sparsely plagioclase microphyric basalt, highly vesicular (~50%; 1–5 mm), incompletely crystallized, with microlitic texture in groundmass. Microphenocrysts of plagioclase (<5%) represented by tabular crystals (0.1–0.3 mm). Groundmass represented by interstitial glass and long plagioclase lathe.	High (~60%); vesicles infilled (from wall to center) with brown-yellow chlorite, brown-green chlorite with zeolites (natrolite and tomsonite), and green clay minerals with traces of zeolites; microphenocrysts of plagioclase partly replaced by albite and chlorite; interstitial glass replaced by opaque minerals and chlorite. Oxidation of basalt is strong (total ~40% of rock).	
39R-2, 114–119	Aphyric basalt, incompletely crystallized, brecciated rock, with microlitic, partly hyaline, texture of groundmass.	~35%; secondary minerals represented by chlorite smectite, and zeolites. Oxidation of basalt is low (total ~3%–5% of rock).	

Table T4 (continued).

Core, section, interval (cm)	Description	Alteration	XRD identification
39R-3, 6–14	Sparsely plagioclase microphyric basalt, weakly vesicular, incompletely crystallized, with microlitic texture. Microphenocrysts of plagioclase (<5%) represented by tabular crystals (0.2–1.2 mm). Groundmass of plagioclase lathe, microlathe of clinopyroxene, opaque minerals, and interstitial glass.	Moderate (~30%); interstitial glass replaced by chlorite and smectite; single vesicles infilled (from wall to center) with chlorite and smectite. Oxidation of basalt is low (total ~2% of rock).	Smectite
43R-2, 84–92	Dacitic tuff. Matrix contains baked ashes.	Very high (80%); secondary minerals represented by chlorite and carbonate. Oxidation of basalt is moderate (total ~10%–15% of rock).	Smectite and quartz in trace amounts with 10% of mica layers
45R-1, 121–126	Plagioclase phyric basalt, vesicular (10%–15%), incompletely crystallized, with microlitic, partly intersertal, texture. Microphenocrysts of plagioclase (10%) are represented by tabular crystals. Groundmass of plagioclase, clinopyroxene, and interstitial glass.	Moderate to high (~40%); olivine completely replaced by chlorite, plagioclase replaced by K-feldspar (adularia?), smectite, chlorite, and carbonate; interstitial glass completely replaced by chlorite and smectite and oxidized Fe; single vesicles infilled with chlorite, smectite, zeolites, and carbonate. Oxidation of basalt is moderate (total ~10%–15% of rock).	Smectite and swelling chlorite and hydromica in trace amounts

Note: XRD = X-ray diffraction.

Table T5. Brief petrographic descriptions of analyzed basalts and X-ray diffraction of secondary minerals from fine fraction removed from altered volcanic rocks, Hole 1138A. (See table note. Continued on next page.)

Core, section, interval (cm)	Description	Alteration	XRD identification
183-1138A-			
78R-1, 60–64	Crystal-lithoclastic tuff.	High (50%–60%); secondary minerals represented by chlorite. Oxidation of basalt is moderate (total ~20% of rock).	Smectite, clinoptilolite, and heulandite
80R-4, 35–40	Aphyric basalt, vesicular (20%–25%; 0.4–3.5 mm), incompletely crystallized, with microdoleritic texture. Rock represented by plagioclase lathe (labradorite-oligoclase) with size 0.1–0.3 mm (40%–45%), small crystals of clinopyroxene (40%–45%), opaque minerals, and glass (5%–10%).	15%–20%; interstitial glass replaced by chlorite; vesicles infilled with chlorite. Oxidation of basalt is very low (total ~1% of rock).	Smectite
81R-1, 34–39	Aphyric basalt, vesicular (10%–15%), incompletely crystallized, with intersertal texture. Rock is represented by plagioclase lathe (40%–45%), clinopyroxene (30%–35%), opaque minerals (5%), and glass (10%).	15%–20%; vesicles infilled with smectite and chlorite with admixture of zeolite in central part of vesicles; veins represented by smectite, chlorite, and zeolite. Rock is nonoxidized.	
81R-2, 51–57	Plagioclase microphyric basalt, weakly vesicular (2%–3%; 0.3–1 mm), incompletely crystallized, with intersertal texture. Microphenocrysts (5%) are tabular plagioclase (labradorite-andesine) (0.2–1.2 mm), single crystals of clinopyroxene (0.2–0.3 mm), and olivine(?). Groundmass is plagioclase (40%–45%), clinopyroxene (30%–35%), opaque minerals (5%), and interstitial glass.	~20%; olivine completely replaced by chlorite; interstitial glass completely replaced by smectite and chlorite; vesicles infilled with smectite and chlorite. Oxidation of basalt is low (~5%).	
82R-2, 76–81	Aphyric basalt, vesicular (10%–15%; up to 10 mm), incompletely crystallized, with microlitic texture. Rock consists of small plagioclase lathe to 0.1 mm, cryptocrystalline clinopyroxene, and glass with opaque minerals.	~20%; vesicles infilled with brown and green chlorite and small crystals of zeolites (natrolite and tomsonite). Oxidation of rock is very low (total ~1%).	
82R-5, 19–23	Aphyric basalt, weakly vesicular, incompletely crystallized, with intersertal texture. Rock consists of small plagioclase lathe (40%–45%; 0.1– to 0.2 mm), isometric crystals of clinopyroxene, opaque minerals (5%), and interstitial glass (10%).	~20%–25%; single vesicles zonally infilled (from wall to center) with chlorite, smectite, and then chlorite. Oxidation of rock is very low.	Smectite
83R-4, 19–24	Aphyric basalt, weakly vesicular, incompletely crystallized, with intersertal texture. Rock is same as Sample 183-1138A-82R-5, 19–23 cm.		Smectite
83R-5, 106–109	Aphyric basalt, vesicular (20%; 0.2–4 mm), incompletely crystallized, with intersertal texture. Rock is same as Sample 183-1138A-82R-5, 19–23 cm, but is more vesicular (20%; 0.2–4 mm).	~30%; vesicles infilled with chlorite, smectite, and admixture chlorite. Oxidation of rock is very low.	
84R-5, 20–25	Sparsely plagioclase microphyric basalt, vesicular (5%–10%; 1.5–7 mm), almost completely crystallized, with intergranular texture. Microphenocrysts (35%–40%), opaque minerals (5%), and interstitial glass (5%). Plagioclase (2%–3%) is represented by tabular crystals (0.2–0.7 mm). Plagioclase is zonal. Groundmass of plagioclase lathe (40%–45%), isometric clinopyroxene.	Moderate (~30%); central parts of zonal plagioclases replaced by mica-type mineral, sometimes with admixture of opaque minerals; interstitial glass completely replaced by chlorite and smectite; vesicles completely infilled with chlorite and smectite, central parts infilled by zeolites, sometimes with admixture of chlorite and opaque minerals. Oxidation of basalt is low.	
86R-1, 130–137	Aphyric basalt, weakly vesicular (2%–3%; 1–1.5 mm), incompletely crystallized, brecciated rock, with microlitic, partly hyaline, texture. Rock consists of plagioclase lathe and brown interstitial glass with opaque minerals.	Moderate (~30%); vesicles infilled with chlorite and smectite, and zeolites. Oxidation of basalt is low (total ~1%–2% of rock).	
86R-2, 21–25	Aphyric basalt, weakly vesicular (30%–35%; 0.1–6 mm), incompletely crystallized, with microlitic, partly hyaline, texture. Rock of long lathe of plagioclase (0.1–0.2 mm) and brown interstitial glass with opaque minerals.	Moderate to high (~ 40%); vesicles infilled (from wall to center) with chlorite and smectite, and zeolites, sometimes vesicles infilled by glass. Oxidation of basalt is low (total ~1% of rock).	
86R-3, 72–74	Aphyric basalt, vesicular (up to 1.5 mm), incompletely crystallized, with intersertal texture. Rock of long lathe of plagioclase, small crystals of clinopyroxene, opaque minerals, and fresh glass.	~10%; walls of vesicles encrusted with chlorite and smectite. Rock is nonoxidized.	
87R-1, 4–9	Plagioclase glomerophyric basalt incompletely crystallized, with microlitictexture. Phenocrysts (5%) of plagioclase (labradorite-oligoclase; to 0.2–0.6 mm and 0.4–2 mm). Groundmass represented by plagioclase, brown interstitial glass, and opaque minerals. Vesicles (~5%).	Low (~10%); phenocrysts of plagioclase partly replaced by chlorite; vesicles infilled with light green chlorite. Rock is nonoxidized.	

Table T5 (continued).

Core, section, interval (cm)	Description	Alteration	XRD identification
87R-2, 76–81	Aphyric basalt, weakly vesicular (<1%; up to 2 mm), incompletely crystallized, with interstitial, partly trachytic, texture. Rock consists of lathe of plagioclase (oligoclase, labradorite-oligoclase), prismatic crystals of clinopyroxene, and brown interstitial glass with opaque minerals.	~20%; interstitial glass partly replaced by chlorite and smectite; vesicles partly or completely infilled with brown-green chlorite and smectite. Oxidation of basalt is low (total ~5%–7% of rock).	
88R-2, 47–53	Aphyric basalt, vesicular (20%–25%; 0.3–7 mm), incompletely crystallized, with vitrophyric-microlitic texture. Rock consists of lathe of plagioclase and brown interstitial glass with opaque minerals.	High (~50%); walls of vesicles encrusted by green-brown chlorite and smectite, then to center vesicles infilled by zeolites (natrolite and tomsonite). Oxidation of basalt is low (total ~3%–5% of rock).	
88R-2, 91–96	Aphyric basalt, vesicular (5%; 0.3–3 mm), incompletely crystallized, with intersertal texture. Rock of lathe of plagioclase, long and isometric crystals of clinopyroxene, and brown interstitial glass.	Moderate (~20%–25%); interstitial glass replaced by chlorite and smectite; vesicles infilled by chlorite and smectite. Oxidation of basalt is very low (total ~1% of rock).	

Note: XRD = X-ray diffraction.

Table T6. Brief petrographic descriptions of analyzed basalts and X-ray diffraction of secondary minerals from fine fraction removed from altered volcanic rocks, Hole 1140A. (See table note. Continued on next page.)

Core, section, interval (cm)	Description	Alteration	XRD identification
183-1140A-			
27R-1, 17–27	Olivine-plagioclase microphyric basalt, weakly vesicular (1%; 0.3 mm), almost completely crystallized, with interstitial texture. Microphenocrysts (5%) of olivine (0.1–0.2 mm) and tabular plagioclase (labradorite; to 0.2–0.5 mm). Groundmass of plagioclase (labradorite-oligoclase; 30%–35% and clinopyroxene (40%–45%) of approximately same size (0.3–0.5 mm, rarely up to 1 mm), opaque minerals (5%), interstitial glass (5%).	10%; olivine completely replaced by chlorite and smectite; interstitial glass replaced by yellow-brown chlorite and opaque minerals; vesicles infilled with brown-yellow chlorite. Oxidation of basalt is very low (total ~1% of rock).	Smectite with 10% of mica layers
27R-1, 63–67	Aphyric basalt, vesicular (5%–10%; 0.1–0.8 mm), incompletely crystallized, with vitrophyric-microlitic texture. Groundmass of plagioclase lathe (0.1–0.3 mm) and brown glass with microlites of clinopyroxene and opaque dust.	5%–10%; vesicles infilled with yellow-green chlorite and carbonate. Oxidation of basalt is low (total ~5% of rock).	
27R-2, 78–23	Sparsely plagioclase-phyric basalt, incompletely crystallized, massive, with intersertal, partly microdoleritic, texture. Phenocrysts of plagioclase (2%), central part of plagioclase represented by labradorite-oligoclase and rim-by oligoclase. Groundmass of long lathe of plagioclase (40%–45%; to 0.2–0.3 mm), clinopyroxene (40%–45%), volcanic glass (10%–15%), and opaque minerals (5%).	10%–15%; labradorite replaced by mica-type mineral; interstitial glass completely replaced by chlorite. Rock is nonoxidized.	Smectite with 20% of mica layers (mixed-layer hydromica-smectite mineral)
31R-1, 9–13	Olivine-clinopyroxene-plagioclase phyric basalt, weakly vesicular (~2%), incompletely crystallized, with intersertal texture. Phenocrysts (20%) represented by plagioclase (central part of plagioclase represented by labradorite-oligoclase and rim-by oligoclase), clinopyroxene of double, olivine as single grains. Groundmass of lathe of plagioclase (to 0.1–0.2 mm), microlites of clinopyroxene, and volcanic glass with opaque minerals.	10%–15%; labradorite replaced by mica-type mineral; vesicles infilled with chlorite. Rock is nonoxidized.	Smectite
31R-1, 76–79	Olivine-clinopyroxene-plagioclase glomerophyric basalt, weakly vesicular (~5%), incompletely crystallized, with intersertal texture. Phenocrysts and microphenocrysts (20%–25%) mainly of plagioclase (labradorite-oligoclase). Groundmass of lathe of plagioclase (35%–40%), microlites of clinopyroxene (30%–35%), and volcanic glass with opaque dust.	~10%; interstitial glass completely replaced by chlorite; vesicles infilled with chlorite and smectite. Rock is nonoxidized.	Smectite with 30% of mica layers (mixed-layer hydromica-smectite mineral); hydromica in trace amount
32R-3, 5–10	Olivine-clinopyroxene-plagioclase phyric basalt, weakly vesicular (~5%; to 0.1–0.3 mm), incompletely crystallized, with intersertal, partly poikilophitic, texture. Phenocrysts and microphenocrysts (20%–25%) of plagioclase, isometric clinophyroxene, and olivine. Groundmass of lathe of plagioclase, microlites of clinopyroxene, and volcanic glass with opaque minerals.	~15%; olivine replaced by smectite and chlorite; interstitial glass completely replaced by chlorite; vesicles infilled with chlorite and smectite. Rock is nonoxidized.	Smectite
32R-4, 17–20	Olivine-clinopyroxene-plagioclase glomerophyric basalt, weakly vesicular (~2%–3%; to 0.1–0.3 mm), incompletely crystallized, with intersertal texture.Phenocrysts and microphenocrysts (30%–35%) mainly of plagioclase (labradorite oligoclase). Groundmass of lathe of plagioclase, microlites of clinopyroxene, and volcanic glass.	~15%–20%; interstitial glass replaced by chlorite and smectite; vesicles infilled with chlorite and smectite. Oxidation of rock is low (total ~4%–5% of rock).	Smectite with 15% of mica layers (mixed-layer hydromica-smectite mineral)
34R-1, 117–121	Olivine-plagioclase glomerophyric basalt, incompletely crystallized, massive, with intersertal texture. Phenocrysts (10%) represented mainly by zoned plagioclase (central part of plagioclase of labradorite and rim-by oligoclase), sometimes plagioclase represented by accretions with olivine. Groundmass of lathe of plagioclase (30%–35%), clinopyroxene (40%–45%), opaque minerals (5%–10%), and interstitial glass (20%–25%).	Moderate (25%–30%); olivine and interstitial glass replaced by chlorite and smectite. Oxidation of rock is very low (total ~2% of rock).	Smectite
34R-3, 100–105	Olivine-plagioclase glomerophyric basalt, incompletely crystallized, massive, with intersertal, partly doleritic, texture. Phenocrysts (5%–10%) of tabular plagioclase (0.2–1.5 mm, sometimes up to 3 mm) and olivine. Groundmass of lathe of plagioclase (30%–35%, size 0.1–0.7 mm), clinopyroxene (30%–35%, size 0.1–0.3 mm), opaque minerals (5%), and interstitial glass (30%–35%).	Moderate (30%–35%); olivine and interstitial glass replaced by chlorite and smectite. Oxidation of rock is low (total ~2%–5% of rock).	Smectite; swelling chlorite in trace amount

Table T6 (continued).

Core, section, interval (cm)	Description	Alteration	XRD identification
35R-1, 35–42	Olivine-clinopyroxene-plagioclase microphyric basalt, weakly vesicular (<1%; 0.05–0.6 mm), incompletely crystallized, with vitrophyric-microlitic texture. Phenocrysts (30%–35%) of olivine (0.1–0.3 mm), clinopyroxene (0.1–0.6 mm), and tabular plagioclase (labradorite, oligoclase; to 0.1–0.7 mm). Groundmass of interstitial glass with long lathe of plagioclase.	10%–15%; olivine replaced by carbonate; interstitial glass replaced by chlorite and smectite; vesicles infilled with chlorite and smectite. Oxidation of rock is low (total ~10%–15% of rock).	
35R-1, 83–87	Olivine-clinopyroxene-plagioclase microphyric basalt, weakly vesicular (3%–5%; 0.05–0.3 mm), incompletely crystallized, with vitrophyric-microlitic texture. Phenocrysts (20%–25%) of olivine (0.1–0.3 mm), clinopyroxene (0.1–0.3 mm to 0.5–1 mm), and tabular plagioclase (labradorite; to 0.1 to 0.8 mm). Groundmass of brown glass with lathe of plagioclase, microlites of clinopyroxene and opaque dust.	8%–10%; olivine replaced by smectite, chlorite, and carbonate; vesicles infilled by smectite, chlorite, and carbonate. Oxidation of rock is low (total ~5% of rock).	
36R-4, 61–67	Olivine-clinopyroxene-plagioclase glomerophyric basalt, weakly vesicular (up to 0.2 mm), incompletely crystallized, with intersertal texture. Phenocrysts (10%–15%) of olivine (0.2 to 0.5–0.7 mm), clinopyroxene (0.4–0.8 mm to 2.5–4.5 mm), and tabular plagioclase (labradorite-oligoclase; 0.15–0.5 mm to 0.9–2.7 mm). Groundmass of lathe of plagioclase (40%–45%), isometric crystals of clinopyroxene (40%–45%), opaque minerals (5%), and intersertal glass (10%–15%).	10%–15%; olivine replaced by smectite and chlorite with opaque minerals; interstitial glass replaced by chlorite and smectite; vesicles infilled by brown-green smectite and chlorite. Oxidation of rock is very low (total ~2% of rock).	
37R-1, 93–99	Olivine-clinopyroxene-plagioclase glomerophyric basalt, weakly vesicular (up to 0.2 mm), incompletely crystallized, with intersertal, partly poikilophitic, texture. Phenocrysts (10%–15%) of olivine (0.2 to 0.5–0.7 mm), clinopyroxene (0.4–0.8 mm to 2.5–4.5 mm), and tabular plagioclase (labradorite-oligoclase; 0.15–0.5 mm to 0.9–2.7 mm). Groundmass of lathe of plagioclase (30%–35%), clinopyroxene (45%–50%), opaque minerals (10%–15%), and intersertal glass (10%–15%).	15%–20%; olivine replaced by smectite and chlorite with opaque minerals; interstitial glass replaced by chlorite and smectite; vesicles infilled by brown-green smectite and chlorite. Rock is nonoxidized.	Smectite with 20%–25% of mica layers (mixed-layer hydromica-smectite mineral); chlorite in trace amount
37R-2, 55–60	Olivine-clinopyroxene-plagioclase phyric basalt, weakly vesicular (up to 0.2 mm), incompletely crystallized, with intersertal, partly subvariolitic, texture. Phenocrysts and microphenocrysts (20%–25%) of olivine (0.1–0.3 mm to 0.8–0.9 mm), clinopyroxene, and tabular plagioclase (labradorite-oligoclase; 0.2–1 mm to 0.9–2.7 mm). Groundmass of intersertal glass with crystals of clinopyroxene, plagioclase, and opaque minerals. They formed subvariolitic accretions.	Low (5%–10%); olivine replaced by smectite, chlorite, and carbonate; interstitial glass partly replaced by chlorite and smectite; vesicles infilled by smectite and chlorite. Rock is nonoxidized.	

Note: XRD = X-ray diffraction.

Table T7. Composition of basalts from Holes 1136A, 1137A, 1138A, and 1140A (Leg 183), and Hole 747C (Leg 120). (Continued on next three pages.)

	183-1136A-					183-1137A-										
Core, section:	15R-2	16R-1	17R-2	18R-2	19R-1	27R-1	29R-1	29R-3	32R-3	32R-7	34R-3	39R-2	39R-3	43R-2	45R-1	78R-1
Interval (cm):	30–36	113–118	84–90	62–67	27–31	100–105	38–43	5–9	71–76	46–50	18–23	114–119	6–14	84–92	121–126	60–64
Piece:	1B	5A	7	4B	4	15	1B	1B	1C	1C	1	9	2		1	
Lab number:	Z-1001	Z-1002	Z-1003	Z-1004	Z-1005	Z-1007	Z-1008	Z-1009	Z-1010	Z-1011	Z-1012	Z-1014	Z-1015	Z-1016	Z-1017	Z-1018
Depth (mbsf):	128.50	138.73	146.22	149.30	157.17	248.60	258.46	259.95	278.77	284.18	297.07	334.64	335.06	353.89	362.91	727.60
Major element oxides (wt%):																
SiO_2	46.50	47.21	48.39	48.59	48.91	47.22	49.29	47.53	48.95	48.59	47.54	51.92	49.20	62.55	48.34	56.83
TiO_2	1.84	1.93	1.79	1.90	1.82	2.66	2.83	2.13	2.03	2.49	4.51	1.75	1.93	0.40	1.84	0.86
Al_2O_3	15.14	14.23	14.40	13.98	13.90	13.79	14.43	13.59	15.60	14.44	13.09	14.15	15.50	13.29	14.12	12.19
Fe_2O_3	9.47	7.87	5.98	5.96	4.48	8.45	5.12	7.52	4.35	5.92	11.51	6.48	6.02	5.78	5.80	7.18
FeO	2.70	3.81	4.83	5.28	7.27	2.37	5	2.27	4.93	5.52	3.75	3.24	4.34	0.57	2.70	0.28
MnO	0.02	0.03	0.10	0.17	0.17	0.11	0.10	0.08	0.11	0.12	0.16	0.26	0.24	0.06	0.28	0.05
MgO	4.54	6.12	6.18	6.19	6.26	6.28	5.54	7.35	5.75	5.74	3.46	4.96	6.02	0.76	3.84	1.79
CaO	7.18	7.65	7.82	8.02	9.39	3.82	8.20	4.46	8.66	8.75	4.16	2.57	5.65	0.56	5.03	2.52
Na_2O	3.39	3.24	3.22	3.19	2.93	3.07	3.22	2.90	3.02	3.08	2.78	2.48	3.22	3.10	0.80	2.16
K_2O	1.19	0.34	0.52	0.22	0.24	2.97	0.76	2.54	0.46	0.49	4.98	5.32	2.00	3.98	8.22	1.00
P_2O_5	0.17	0.14	0.19	0.19	0.17	0.36	0.35	0.28	0.28	0.33	0.74	0.32	0.31	0.07	0.23	0.14
H_2O^+	1.58	1.28	1.25	1.19	0.90	2.03	0.79	3.03	1.20	0.19	0.72	0.99	0.76	2.19	2.03	3.95
H_2O^-	4.71	4.77	4.06	4.02	2.69	5.11	3.36	4.48	3.36	3.82	2.04	4.17	4.34	5.63	3.19	9.96
CO_2	1.32	0.65	0.43	0.21	<0.2	0.40	<0.2	0.84	0.29	0.33	<0.2	0.41	0.28	0.79	3.67	<0.2
Others:		0.27	0.30	0.34	0.31	0.82	0.40	0.36	0.51	0.05	0.30	0.89	0.06	0.24		0.89
Total:	99.75	99.54	99.46	99.45	99.45	99.46	99.39	99.36	99.50	99.86	99.74	99.91	99.87	99.97	100.09	99.80
Fe_2O_3/FeO	3.51	2.07	1.24	1.13	0.62	3.57	1.02	3.31	0.88	1.07	3.07	2.00	1.39	10.14	2.15	25.64
Density (g/cm^3):	2.08	2.52	2.59	2.59	2.75	2.11	2.75	2.33	2.63	2.65	2.49	2.28	2.55	1.81	2.32	1.46
Trace elements (ppm):																
La	7.7	8.4	11	10	8.7	27	25	18	18	23	110	25	25	190	15	47
Ce	17	19	22	21	19	59	55	37	40	50	180	50	50	410	31	100
Nd	12	13	16	15	14	32	31	22	22	27	78	27	28	160	18	51
Sm	3.9	4.1	5.1	4.5	4.4	7.8	7.3	5.7	5.7	7.1	16	6.3	7.1	29	4.5	11
Eu	1.4	1.4	1.7	1.6	1.5	2.4	2.3	1.8	1.8	2.2	3.6	2	2.1	2.1	1.4	2
Tb	0.93	1	1.3	1.1	0.97	1.2	1.1	0.93	1	1.1	2.2	1.1	1.1	3.6	0.8	2.3
Yb	2.1	2.3	2.9	2.9	2.7	2.4	2.3	2	1.9	2.3	4.3	2.2	2.6	6.4	1.7	6.9
Lu	0.34	0.39	0.49	0.45	0.46	0.39	0.37	0.31	0.3	0.34	0.67	0.34	0.4	0.92	0.25	1.1
Sc																
Cr	275	215	200	185	185	73	84	160	160	150	220	98	97	30	170	30
Ni	62	74	61	64	56	32	40	45	50	47	67	30	37	22	43	30
V	497	320	317	347	282	290	310	230	270	307	215	302	292	98	215	177
Co	39	47	40	42	35	34	40	37	35	37	23	23	28	13	24	20
Cu	30	135	90	120	133	43	52	40	47	66	56	40	55	40	59	59
Pb	6	5	6	6	5	7	8	6	7	7	21	8	7	33	7	10
Zn	88	83	85	93	93	94	125	98	83	97	83	87	92	130	77	88
Sn	3.8	3.8	3.3	3.5	3	3.3	3.6	3.3	3.4	3.3	4.4	2.7	3	5.1	2.5	5
Nb	5.5	5.8	6.8	7.1	6.3	18	15	12	13	14	49	12	13	68	11	40
Zr	96	87	108	104	100	240	230	170	170	200	570	180	200	620	165	300
Y	25	28	34	29	29	36	33	24	25	30	52	35	31	69	25	54
Rb	31	4.9	4.7	3.8	2.6	35	6.2	30	7.7	3.3	91	75	24	83	120	40
Sr	240	220	240	240	220	440	550	510	540	550	660	250	410	79	580	540
Ba	62	68	86	84	49	290	240	310	220	190	360	250	210	24	320	100
Th	1.1	<1	1.6	1.3	2.2	4.4	2.8	2	2.3	3.3	8.2	4.3	3.8	27	3.1	7.4

Notes: Others = loss on ignition (LOI) – (H_2O^+ + H_2O^- + CO_2). — = below the sensitivity of the analytical method.

Table T7 (continued).

	183-1138A-											183-1140A-						
Core, section:	80R-4	81R-1	81R-2	82R-2	82R-5	83R-4	83R-5	84R-5	86R-3	88R-2	88R-2	27R-1	27R-1	27R-2	31R-1	31R-1	32R-3	32R-4
Interval (cm):	35–40	34–39	51–57	76–81	19–23	19–24	106–109	20–25	72–74	47–53	91–96	17–27	63–67	78–83	9–13	76–79	5–10	17–20
Piece:	2A	4A	2A	9	4	1	9	1C	8	2A	4	1A	4	3B	1	5	2	2
Lab number:	Z-1019	Z-1020	Z-1021	Z-1022	Z-1023	Z-1024	Z-1025	Z-1026	Z-1029	Z-1032	Z-1033	Z-1034	Z-1035	Z-1036	Z-1037	Z-1038	Z-1039	Z-1040
Depth (mbsf):	751.05	756.24	757.82	767.86	771.73	779.70	781.99	790.03	807.82	825.28	825.72	239.47	239.93	241.49	270.59	271.26	278.25	279.83
Major element oxides (wt%):																		
SiO_2	46.18	48.24	46.75	52.27	47.06	47.46	47.74	47.82	46.73	47.16	44.91	47.39	46.83	46.68	47.67	48.69	48.30	47.38
TiO_2	1.99	1.91	2.11	2.08	2.32	2.19	1.97	1.93	2.24	2.68	2.74	1.21	1.10	1.12	2.05	2.23	3.14	1.10
Al_2O_3	14.48	13.39	14.19	11.25	12.75	13.03	13.97	13.97	12.72	11.30	12.12	14.71	14.32	14.44	15.51	14.94	13.52	15.26
Fe_2O_3	9.88	7.83	5.54	7.57	5.19	3.89	5.41	6.65	6.55	9.87	9.54	4.83	6.36	6.12	5.61	3.93	4.42	7.83
FeO	3.28	4.30	6.70	4.43	8.53	9.65	6.60	7.41	9.30	4.80	7.84	7.16	5.92	6.02	5.37	7.13	8.32	3.25
MnO	0.19	0.13	0.26	0.12	0.25	0.24	0.12	0.32	0.34	0.26	0.33	0.05	0.18	0.16	0.18	0.17	0.13	0.10
MgO	6.39	6.28	5.99	5.26	6.28	5.84	6.28	6.08	5.56	5.71	5.86	6.48	7.10	8.15	5.45	5.84	5.43	6.57
CaO	9.15	8.73	10.70	7.77	10.31	10.38	9.66	10.34	7.45	8.39	8.04	11.79	11.76	11.16	11.11	10.82	9.51	10.56
Na_2O	2.66	2.58	2.65	2.27	2.79	2.86	2.86	2.87	4.08	2.86	2.92	2.54	2.60	2.60	2.78	3.00	3.08	2.64
K_2O	0.23	0.85	0.39	1.57	0.19	0.21	0.42	0.29	0.37	1.29	0.59	0.13	0.44	0.11	0.58	0.36	0.52	0.81
P_2O_5	0.21	0.21	0.20	0.16	0.25	0.27	0.27	0.27	0.33	0.24	0.37	0.12	0.11	0.59	0.29	0.23	0.34	0.13
H_2O^+	0.36	1.30	0.95	1.52	0.64	0.52	1.29	0.30	2.33	4.96	1.54	1.36	1.02	1.39	0.91	0.87	0.93	1.65
H_2O^-	4.49	3.90	2.83	3.55	2.86	2.62	2.44	1.82	1.65	5.31	2.97	1.28	1.18	1.44	1.44	1.50	1.64	1.96
CO_2	<0.2	0.34	0.26	0.26	0.31	0.22	<0.2	<0.2	<0.2	<0.2	<0.2	<0.2	0.38	<0.2	<0.2	<0.2	<0.2	<0.2
Others:	0.47		0.11			0.26		0.04	0.35	0.01	0.09	0.31	0.41	0.07	0.64	0.13	0.12	0.39
Total:	99.96	99.99	99.63	100.08	99.73	99.64	99.03	100.11	100.00	100.04	98.86	99.36	9.71	100.05	99.59	99.84	99.40	99.63
Fe_2O_3/FeO	3.01	1.82	0.83	1.71	0.61	0.40	0.82	0.90	0.70	2.06	1.22	0.67	1.07	1.02	1.04	0.55	0.53	2.41
Density (g/cm^3):	2.50	2.34	2.53	2.47	2.44	2.62	2.20	2.63	2.49	1.96	2.29	2.90	2.89	2.88	2.62	2.73	2.55	2.83
Trace elements (ppm):																		
La	10	12	12	14	13	15	16	16	18	29	35	3.8	4.1	3.7	13	14	20	4
Ce	24	23	27	28	30	32	38	41	46	69	81	8.2	11	10	32	33	49	11
Nd	15	15	16	16	18	19	24	24	27	40	49	8.5	10	9	21	21	30	8.4
Sm	3.7	3.9	4.5	4.4	4.8	5.3	6.5	6	7.6	11	13	3.6	3.8	3.5	5.9	5.4	8.4	2.8
Eu	1.4	1.4	1.6	1.4	1.6	1.6	1.9	2	2.4	2.6	3.2	1.3	1.3	1.3	2	2	2.6	1.2
Tb	0.83	0.81	0.95	1	0.97	0.99	1.2	1.1	1.4	1.7	1.9	0.83	0.96	0.86	0.99	1.2	1.4	0.84
Yb	2.3	2.6	3.2	2.9	3.3	3.8	3.4	3.2	4.1	6	6.1	2.8	2.8	2.5	2.8	2.9	3.5	2.4
Lu	0.41	0.42	0.5	0.46	0.54	0.61	0.56	0.51	0.63	0.94	0.93	0.4	0.39	0.39	0.39	0.41	0.46	0.38
Sc																		
Cr	98	80	98	63	73	88	90	64	51	30	30	265	275	295	103	150	67	270
Ni	58	62	66	38	56	53	56	49	37	36	38	92	84	102	49	73	46	104
V	370	405	530	287	440	395	487	415	355	430	497	305	297	310	350	372	397	352
Co	41	40	48	25	48	44	50	44	41	34	45	50	37	59	36	47	42	50
Cu	160	145	135	140	170	170	135	150	245	260	245	170	140	160	135	145	145	210
Pb	<5	6	6	5	7	6	7	6	7	7	8	6	5	5	6	6	6	5
Zn	79	88	107	83	108	122	108	123	122	128	170	93	88	93	102	160	137	92
Sn	3.8	3	3.8	1.9	3.9	4.2	4.4	3.4	2.7	3	5.1	3.4	3.4	2.5	3.4	3	3.8	2.5
Nb	9.4	9.5	10	11	12	12	14	13	18	22	19	3.6	2.7	3.6	3	11	13	20
Zr	120	110	120	130	150	160	170	170	230	260	250	81	78	78	76	160	170	230
Y	24	30	30	32	36	40	41	39	45	57	58	29	32	29	32	33	43	26
Rb	4.2	10	4.4	23	1.9	1.4	5.2	1.1	4.5	21	7.8	<1	9.2	1.5	7.9	2.5	5.7	12
Sr	210	470	205	370	220	200	260	210	190	610	190	130	130	120	250	260	250	110
Ba	82	89	77	88	44	35	56	82	46	160	61	54	29	48	93	120	150	11
Th	1.8	<1	1.6	<1	2.1	<1	1.2	2.3	2.2	1.7	3.4	<1	1	1.1	1.4	1.9	2.3	1.6

Table T7 (continued).

	183-1140A-							120-747C-										
Core, section:	34R-1	34R-3	35R-1	35R-1	36R-4	37R-1	37R-2	12R-1	37591.00	37592.00	12R-2	37593.00	12R-3	13-1	13-1	13R-3	14R-1	15R-1
Interval (cm):	117–121	100–105	35–42	83–87	61–67	93–99	55–60	53–56	125–127	6–9	85–87	18–22	146–148	6–10	98–102	97–99	49–51	22–24
Piece:	4D	3	2A	4	2D	1D	2A	7A	18	1	10	3A	12	1A	2D	10B	3C	3A
Lab number:	Z-1041	Z-1042	Z-1043	Z-1044	Z-1045	Z-1046	Z-1047	Z-91	Z-629	Z-630	Z-92	Z-631	Z-93	Z-632	Z-633	Z-94	Z-95	Z-96
Depth (mbsf):	295.27	297.78	303.85	304.33	317.52	318.23	318.97	303.53	304.25	304.56	305.35	306.18	307.46	312.56	313.48	316.47	322.49	331.72
Major element oxides (wt%):																		
SiO_2	47.30	47.00	47.62	48.66	48.11	49.05	48.24	45.79	45.00	45.80	43.82	48.16	47.94	48.90	47.44	44.65	45.60	44.91
TiO_2	1.15	1.11	1.35	1.30	1.18	1.23	1.07	2.19	1.76	1.67	1.59	1.49	1.81	1.53	1.57	2.29	1.86	1.26
Al_2O_3	15.40	15.88	14.82	14.30	14.10	14.93	14.53	18.55	15.53	14.47	14.38	14.48	15.66	14.81	15.45	16.87	15.29	15.78
Fe_2O_3	4.55	6.77	6.41	4.75	4.23	4.39	5.65	8.77	8.89	5.83	7.74	6.38	4.22	4.96	8.99	8.33	7.73	6.92
FeO	6.62	2.93	6.34	6.50	6.72	6.11	6.19	1.19	2.08	3.61	4.75	5.02	4.97	5.62	2.44	3.12	3.86	3.01
MnO	0.16	0.09	0.14	0.14	0.13	0.14	0.17	0.20	0.22	0.24	0.02	0.14	0.05	0.18	0.13	0.02	0.15	0.08
MgO	7.23	8.27	6.74	6.07	7.64	6.32	6.51	4.45	5.51	6.60	8.51	7.08	7.24	6.63	6.12	6.71	7.71	7.98
CaO	10.55	10.18	11.85	12.24	11.66	12.05	12.34	4.68	5.94	9.55	8.84	9.80	11.76	11.43	8.14	7.68	9.99	8.57
Na_2O	2.60	2.63	2.73	2.82	2.76	2.82	2.79	3.08	1.80	2.03	2.70	2.44	3.42	2.40	2.58	3.12	2.91	2.61
K_2O	0.08	0.36	0.45	0.51	0.11	0.11	0.16	1.68	1.93	0.98	0.66	0.56	0.75	0.33	0.79	1.22	0.84	1.22
P_2O_5	0.11	0.11	0.12	0.12	0.12	0.12	0.13	0.18	0.11	0.19	0.17	0.17	0.16	0.20	0.16	0.22	0.18	0.14
H_2O^+	1.40	1.99	0.74	0.68	1.00	0.42	0.55	3.56	3.56	2.81	2.30	1.35	0.69	0.57	1.57	1.65	1.23	2.93
H_2O^-	2.26	2.25	0.67	0.60	1.72	1.58	1.04	5.20	5.17	3.13	3.65	1.97	1.69	1.54	2.90	3.72	2.56	3.91
CO_2	<0.2	<0.2	<0.2	0.61	<0.2	<0.2	<0.2	—	1.67	2.17	—	0.25	—	0.40	0.46	—	—	—
Others:	0.04	0.29	0.09	0.19	0.04	0.12	0.32	0.06	0.87	0.30		0.13		0.44	0.65			
Total:	99.45	99.86	100.07	99.49	99.52	99.39	99.69	99.58	100.04	99.38	99.13	99.42	100.36	99.94	99.39	99.60	99.91	99.32
Fe_2O_3/FeO	0.69	2.31	1.01	0.73	0.63	0.72	0.91	7.37	4.27	1.61	1.63	1.27	0.85	0.88	3.68	2.67	2.00	2.30
Density (g/cm^3):	2.57	2.57	2.93	2.87	2.95	2.80	2.88	1.96		2.44	2.59	2.60	2.76	2.76	2.54	2.50	2.60	2.55
Trace elements (ppm):																		
La	3.9	3.6	4	4.3	3.9	4.6	4.4	14	9.2	12	11		13			19	17	13
Ce	9.4	11	11	13	12	14	13	29	24	26	24		25			35	33	27
Nd	8.2	8.4	9.6	10	9	11	11		14	16								
Sm	3	3	3.6	3.5	3.1	3.4	3.4	4.5	3.4	3.9	3.8		4.2			5.8	4.9	3.7
Eu	1.1	1.1	1.3	1.4	1.3	1.3	1.3	1.6	1.2	1.3	1.4		1.5			1.9	1.5	1.2
Tb	0.74	0.81	0.94	0.85	0.85	0.85	0.84	0.79	0.62	0.79	0.68		0.8			1	0.87	0.61
Yb	2.4	2.3	2.7	2.6	2.2	2.5	2.6	2.1	2	2	2.2		2.2			3.4	2.8	2.1
Lu	0.38	0.37	0.43	0.44	0.34	0.41	0.42	0.28	0.33	0.29	0.34		0.36			0.52	0.42	0.32
Sc								57			46		48			46	46	39
Cr	275	320	170	180	200	180	200	400	345	285	270	245	240	245	255	60	95	405
Ni	84	96	65	46	64	66	82	95	76	75	80	64	85	65	62	90	100	135
V	377	350	317	352	337	362	372	540	425	357	320	312	250	312	367	240	270	175
Co	62	54	49	39	54	55	64	55	52	52	50	52	50	48	49	60	55	55
Cu	160	155	170	165	170	185	185	55	100	90	100	107	100	125	140	45	60	40
Pb	5	6	6	5	6	6	5	6	<5	7	<5	<5	<5	<5	6	<5	<5	<5
Zn	93	91	77	100	93	97	100	95	72	86	95	94	95	86	86	115	115	90
Sn	3.6	3.5	3.3	3.3	3.6	3.8	3		2.5	2.7		2.5		2.4	2.5			
Nb	3.9	2.1	3.6	3.9	2.5	4.3	3.9	11	9	7.9	9	6.9	8.7	9.1	7.9	13	10	7.6
Zr	72	64	77	77	75	78	76	100	120	120	95	120	130	110	120	150	91	87
Y	26	25	29	31	28	28	28	27	19	26	30	25	27	26	29	29	26	20
Rb	<1	4.9	9	9.3	<1	<1	1.1	29	55	21	6.3	6.1	2.7	3.6	9.2	13	6.4	12
Sr	110	110	120	120	130	120	120	190	120	160	230	290	280	240	220	250	190	210
Ba	48	27	28	37	45	29	31	120	100	110	140	120	130	120	110	290	210	150
Th	<1	<1	<1	1.4	1.2	<1	<1		<1	1.6		2.5		1.8	<1			

Table T7 (continued).

	120-747C-					
Core, section:	15R-2	16R-2	16-2	16R-4	16-5	16-5
Interval (cm):	97–99	51–53	101–105	14–16	0-3	105-108
Piece:	13	1D	1G	1A	1A	
Lab number:	Z-97	Z-98	Z-635	Z-99	Z-637	Z-638
Depth (mbsf):	333.97	343.01	343.51	345.64	347.00	348.05
Major element oxides (wt%):						
SiO_2	44.30	46.75	47.02	45.10	47.80	47.64
TiO_2	1.53	1.25	1.06	1.36	1.18	1.09
Al_2O_3	12.79	14.34	15.80	13.36	15.88	16.02
Fe_2O_3	8.62	7.58	6.63	6.17	3.89	6.81
FeO	3.44	3.10	3.21	4.47	5.06	3.39
MnO	0.08	0.05	0.17	0.17	0.10	0.13
MgO	9.91	7.79	7.54	10.33	7.93	6.90
CaO	8.89	9.96	9.30	10.69	10.87	9.10
Na_2O	2.13	2.13	2.15	2.32	2.32	1.92
K_2O	0.89	2.09	1.50	1.36	0.44	1.90
P_2O_5	0.13	0.10	0.15	0.10	0.17	0.14
H_2O^+	5.14	2.56	2.61	2.66	1.38	2.59
H_2O^-	2.57	2.84	1.93	2.38	1.90	1.73
CO_2	—	—	0.39	—	0.38	0.46
Others:			0.07		0.14	0.02
Total:	100.42	100.54	99.53	100.47	99.44	99.84
Fe_2O_3/FeO	2.51	2.44	2.07	1.38	0.77	2.01
Density (g/cm^3):	2.55	2.59	2.57	2.67	2.67	2.90
Trace elements (ppm):						
La	10	14		14		
Ce	22	30		24		
Nd						
Sm	3.5	3.9		3.7		
Eu	1.1	1.2		1.2		
Tb	0.62	0.67		0.68		
Yb	1.8	2		2		
Lu	0.28	0.31		0.31		
Sc	40	36		38		
Cr	425	430	340	290	320	360
Ni	135	115	105	115	93	74
V	220	165	257	155	220	220
Co	55	40	51	40	51	46
Cu	45	35	52	80	80	52
Pb	<5	<5	<5	<5	<5	<5
Zn	90	80	80	80	77	68
Sn			2.6		2.5	2.3
Nb	8.2	7	6.7	7.3	8.6	7.5
Zr	88	52	100	92	99	98
Y	22	21	22	20	19	22
Rb	11	17	13	9.6	1.7	15
Sr	190	160	240	250	260	220
Ba	110	210	130	120	130	200
Th			1.6		1.2	1.4

Table T8. Secondary minerals within basement units identified by X-ray diffraction, Hole 1136A.

Core, section, piece, interval (cm)	Unit	Lab number	Description	XRD identification
183-1136A-				
15R-2 (1B, 30–36)	1	Z-1001-2	Vesicle filling (dark blue clay).	Iron hydromica with ~5% of swelling layers and smectite with ~15% of mica-type layers
		Z-1001-3	Vein	Calcite
16R-1 (5A, 113–118)		Z-1002-2	Brown clay on the open joint	Smectite
17R-2 (7, 84–90)	2	Z-1003-2	Vesicle filling (light brown clay)	Smectite and heulandite
		Z-1003-3	Black clay on the open joint	Heulandite and smectite
18R-2 (4B, 62–67)		Z-1004-2	Vesicle filling	Smectite

Note: XRD = X-ray diffraction.

Table T9. Secondary minerals within basement units identified by X-ray diffraction, Hole 1137A.

Core, section, piece, interval (cm)	Unit/Subunit	Lab number	Description	XRD identification
183-1137A-				
25R-4 (4, 100–115)	2A	Z-1006-2	Vein	Calcite and traces of clinoptilolite and quartz
27R-1 (15, 100–115)	3A	Z-1007-2	Vesicle filling	Smectite and 7.2-Å mineral (dickite?)
		Z-1007-3	Vesicle filling	Calcite and smectite and 7-Å mineral (dickite?), traces of 8.9-Å zeolite
29R-3 (1B, 5–9)	4	Z-1009-2	Vesicle filling (dark blue clay)	Smectite
		Z-1009-3	Vesicle filling	Smectite and clinoptilolite and traces of 7-Å mineral
32R-7 (1C, 46–50)		Z-1011-2	Vesicle filling (black clay)	Smectite and traces of heulandite
34R-3 (1, 18–23)	6	Z-1012-2	Green matter on the contact of basalt and tuff	Mixed-layer illite-smectite mineral with mica-type layers (20%–50%) and traces of hydromica with ~5% of swelling layers; quartz
37R-5 (1D, 73–79)	7A	Z-1013-2	Vesicle filling (dark blue clay)	Smectite and mixed-layer smectite-chlorite mineral and traces of 8.9-Å zeolite
		Z-1013-3	Vein	Quartz, clinoptilolite, and smectite
		Z-1013-4	Grayish yellow patches with white matter	Smectite and clinoptilolite
39R-2 (9, 114–119)	8A	Z-1014-2	Vesicle filling (black clay)	Smectite, chlorite, and defective chlorite and traces of hydromica and quartz
		Z-1014-3	Vesicle filling and veins (blue matter)	Smectite, hydromica, chlorite, and mixed-layer chlorite-smectite mineral
39R-3 (2, 6–14)		Z-1015-2	Vesicle filling (black clay)	Chlorite and smectite with ~10%–15% mica layers.
		Z-1015-3	Large 1-cm vesicle (black clay)	Smectite and traces of defective chlorite

Note: XRD = X-ray diffraction.

Table T10. Secondary minerals within basement units by X-ray diffraction, Hole 1138A.

Core, section, piece, interval (cm)	Unit	Lab number	Description	XRD identification
183-1138A-				
80R-4 (2A, 35–40)	5	Z-1019-2	Vesicle filling (black clay)	Smectite and traces of both heulandite(?) and serpentine(?)
81R-1 (4A, 34–39)	6	Z-1020-2	Vesicle filling (white and blue matter)	Clinoptilolite and smectite, traces of hydromica
		Z-1020-3	Vesicle filling (black matter)	Heulandite, clinoptilolite, smectite, and traces of chlorite
		Z-1020-4	Vesicle filling or veins (white matter)	Mordenite, clinoptilolite, smectite, and traces of hydromica1
		Z-1020-5	Vesicle filling (black clay)	Smectite, defective chlorite, and traces of clinoptilolite and hydromica
81R-2 (2A, 51–57)	6	Z-1021-2	Vesicle filling (black clay)	Smectite, traces of chlorite and defective chlorite
82R-2 (9, 76–81)	9	Z-1022-2	Vesicle filling or veins (gray and white matter)	Smectite, clinoptilolite, and traces of quartz
82R-5 (4, 19–23)	9	Z-1023-2	Vesicle filling (black clay)	Smectite and traces of hydromica
83R-4 (1, 19–24)	10	Z-1024-2	Vesicle filling (black clay)	Smectite
83R-5 (9, 106–109)	11	Z-1025-2	Large vesicles (white matter on walls)	Smectite
		Z-1025-3	Clinoptilolite and traces of smectite	Smectite
84R-5 (1C, 20–25)	13	Z-1026-2	Vesicle filling (black clay)	Smectite and clinoptilolite-heulandite
		Z-1026-4		Smectite and clinoptilolite-heulandite
86R-1 (13, 130–137)	17	Z-1027-2	Vesicle filling	Heulandite, magnetite, and Fe-Zn-spinel(?)
		Z-1027-3	Vesicle filling	Smectite, heulandite, traces of clinoptilolite, magnetite, and Fe-Zn-spinel(?)
		Z-1027A	Central parts of veins and vesicles	Stilbite and heulandite-clinoptilolite
		Z-1027B	Vesicle and vein	Heulandite-clinoptilolite
		Z-1027C	Vesicle filling	Smectite, heulandite, and analcime
		Z-1027D	Vesicle filling	Analcime, clinoptilolite, and smectite
86R-3 (8, 72–74)	17	Z-1029-2	Vesicle filling (black clay)	Smectite, traces of defective chlorite, serpentine(?), and natrolite(?)
87R-1 (1, 4–9)	19	Z-1030-2	Vesicle and vein (dark clay)	Smectite, heulandite, traces of magnetite, and Fe-Zn-spinel(?)
		Z-1030A	Central part of vein	Analcime, stilbite, clinoptilolite, or heulandite
		Z-1030B	Vesicle filling	Clinoptilolite or heulandite, and smectite
87R-2 (13, 76–81)	19	Z-1031-2	Vesicle filling (black clay)	Smectite and traces of hydromica
88R-2 (2A, 47–53)	19	Z-1032-2	Vesicle and vein filling (dark clay)	Heulandite-clinoptilolite and smectite
88R-2 (4, 91–96)	21	Z-1033-2	Vesicle filling (black clay)	Smectite and traces of heulandite
		Z-1033A	Vesicle filling	Heulandite-clinoptilolite and smectite

Note: XRD = X-ray diffraction.

Table T11. Microprobe analyses of clay minerals and zeolites in basalts, Hole 1138A.

	183-1138A-																		
Core, section:	86R-2		87R-1																
Piece, interval (cm):	(3, 21–25)		(1, 4–9)																
Number:	1	2	3	4	5	6	7	8	9	10	11	12	13	14	15	16	17	18	19
Major element oxides (wt%):																			
SiO_2	67.90	70.70	67.13	67.92	61.43	61.93	60.36	62.21	63.15	70.21	62.53	66.96	62.61	63.33	62.35	60.62	63.05	64.16	69.04
Al_2O_3	14.77	14.18	14.63	13.90	18.19	17.16	18.53	16.84	16.22	15.82	17.98	17.43	17.48	16.65	14.46	18.26	16.65	15.84	15.25
FeO*	0.26	1.15	0.39	0.25	0.16	0.00	0.01	0.00	0.10	0.29	0.02	0.00	0.02	0.00	0.02	0.09	0.00	0.01	0.08
CaO	4.57	4.15	4.85	4.71	8.41	5.95	8.27	5.87	5.14	5.25	8.24	8.72	8.04	8.38	5.72	8.15	5.57	5.32	4.55
MgO	0.01	0.01	0.16	0.00	0.00	0.00	0.00	0.00	0.00	0.03	0.00	0.00	0.00	0.00	0.00	0.00	0.00	0.01	0.00
Na_2O	0.20	0.53	0.94	1.32	0.68	0.90	1.00	1.42	1.34	1.18	0.26	0.12	0.22	0.31	1.85	0.24	0.83	0.67	0.39
K_2O	0.29	0.47	0.13	0.15	0.05	0.43	0.03	0.42	0.42	0.22	0.03	0.05	0.06	0.05	0.39	0.06	0.41	0.41	0.42
Total:	88.01	90.19	88.23	88.26	88.78	86.37	88.2	86.76	86.3	92.99	89.06	93.28	88.42	88.71	84.8	87.44	86.51	86.43	89.73

Notes: FeO* = total FeO as Fe_2O_3 + FeO. 1 = vesicle, finely crystalline zeolite mass; 2 = vesicle, zeolite; 3 = vesicle, central part of the finely crystalline zeolite; 4 = radiated zeolite; 5–8 = zeolites from vesicle; 9, 10 = vesicle, (9) coarsely crystalline stilbite, (10) small striated crystals of heulandite; 11–14 = vesicle filled with crystals of stilbite; 15–18 = vesicle filled with (15, 18) heulandite in its peripheral parts and (16, 17) stilbite in its central part; 19–22 = crack filled with smectite in the outer part; innermost crack is filled with (21, 22) cryptocrystalline zeolite, (20) finely crystalline stilbite from crack centerward; 23, 24 = (23) finely and (24) coarsely crystalline zeolite (thomsonite) from vesicle; 25 = radiated strongly birefringent zeolite (mordenite) from vesicle; 26, 27 = finely crystalline aggregate of zeolite (thomsonite) from vesicle; 28, 29 = (28) large crystal of heulandite (29) surrounded with cryptocrystalline zeolite mass; 30–34 = vesicle filled in peripheral parts with (33) smectite, (32, 34) fine cryptocrystalline zeolites, and (30, 31) large crystals of stilbite; 35 = cryptocrystalline zeolite in center of vesicle; 36, 37 = large crystalline zeolite from center of vesicle.

Table T11 (continued).

	183-1138A-																		
Core, section:	88R-2			86R-2							86R-2								
Piece, interval (cm):	(4, 91–96)			(3, 21–25)							(3, 21–25)								
Number:	20	21	22	23	24	25	26	27	28	29	30	31	32	33	34	35	36	37	
Major element oxides (wt%):																			
SiO_2	67.21	64.86	61.39	40.12	40.76	71.32	39.63	38.96	66.50	62.56	63.22	69.52	66.23	32.26	64.53	68.85	67.52	68.32	
Al_2O_3	13.64	15.47	15.94	30.31	29.03	15.32	29.45	29.77	17.44	17.73	16.24	13.36	14.27	8.77	16.89	13.62	14.27	13.40	
FeO*	0.19	0.03	0.05	1.22	1.21	0.32	0.93	0.64	0.03	0.19	0.02	0.05	0.67	21.41	0.23	0.11	0.44	0.26	
CaO	4.08	5.00	5.31	11.74	11.69	4.26	12.04	12.47	5.31	6.80	5.74	4.00	4.85	1.19	8.98	4.08	4.98	4.20	
MgO	0.02	0.04	0.01	0.50	0.44	0.00	0.19	0.24	0.00	0.00	0.01	0.00	0.02	7.74	0.00	0.02	0.00	0.01	
Na_2O	1.11	0.34	0.52	2.86	2.64	0.52	3.38	3.14	0.27	0.33	2.13	2.16	2.90	1.47	0.58	2.21	0.41	1.98	
K_2O	0.44	0.41	0.44	0.04	0.13	0.26	0.03	0.03	0.40	0.35	0.32	0.30	0.30	0.60	0.03	0.17	0.25	0.29	
Total:	86.7	86.15	83.66	86.79	85.91	91.71	85.64	85.27	89.96	87.95	87.67	89.4	89.24	73.53	91.25	89.07	87.88	88.48	

Table T12. Secondary minerals within basement units identified by X-ray diffraction, Hole 1140A.

Core, section, piece, interval (cm)	Unit	Lab number	Description	XRD identification
183-1140A-				
27R-1, (1A, 17–27)	1	Z-1034-2	Dark green clay on the open joint	Smectite and defective chlorite
27R-1, (4, 63–67)		Z-1035-2	White vein in glass	Calcite
32R-3, (2, 5–10)	3	Z-1039-2	Vesicle filling (gray-green clay)	Smectite
36R-4, (2D, 61–67)	6	Z-1045-2	Black clay on the open joint	Smectite and traces of serpentine(?) and quartz

Note: XRD = X-ray diffraction.

Table T13. Abundance of major and trace elements (g/1000 cm³) in igneous rocks, Holes 1136A, 1137A, 1138A, and 1140A. (Continued on next two pages.)

Hole:	183-1136A-					183-1137A-									
Core, section:	15R-2	16R-1	17R-2	18R-2	19R-1	27R-1	29R-1	29R-3	32R-3	32R-7	34R-3	39R-2	39R-3	43R-2	45R-1
Interval (cm):	30–36	113–118	84–90	62–67	27–31	100–105	38–43	5–9	71–76	46–50	18–23	114–119	6–14	84–92	121–126
Piece:	1B	5A	7	4B	4	15	1B	1B	1C	1C	1	9	2		1
Lab number:	Z-1001	Z-1002	Z-1003	Z-1004	Z-1005	Z-1007	Z-1008	Z-1009	Z-1010	Z-1011	Z-1012	Z-1014	Z-1015	Z-1016	Z-1017
Depth (mbsf):	128.5	138.73	146.22	149.3	157.17	248.6	258.46	259.95	278.77	284.18	297.07	334.64	335.06	353.89	362.91
Major elements (g/1000 cm³):															
Si	475	586	614	616	650	493	659	545	626	626	566	578	614	561	541
Ti	24.1	30.8	29.1	30.9	31	35.7	48.6	31.4	33.3	41.2	68.9	25	30.9	4.6	26.4
Al	175	200	207	201	209	163	219	177	226	211	177	178	219	135	179
Fe (sum)	191	225	215	224	250	173	214	172	188	233	279	168	202	86	147
Mn	0.3	0.6	2.1	3.6	3.7	1.9	2.2	1.5	2.3	2.6	3.2	4.8	5	0.9	5.2
Mg	59.9	98.1	101	101	107	84.7	95.7	109	94.8	95.5	53.2	71.2	96.9	8.8	55.4
Ca	112	145	152	156	191	61	168	78.3	169	173	75.8	43.7	108	7.7	86.1
Na	55	63.9	64.9	64.2	61.8	52.5	62.4	54.3	62.6	55.9	47.9	57	62.2	11.1	0
K	21.6	7.5	11.7	5	5.7	55.1	18.1	51.8	10.4	11.2	105	105	44.3	63.4	163
P	1.6	1.6	2.3	2.3	2.1	3.5	4.4	3	3.3	4	8.2	3.3	3.6	0.6	2.4
Minor elements (g/1000 cm³ × 10⁻³):															
La	16	21.2	28.5	25.9	23.9	57	68.8	41.9	47.3	61	274	57	63.8	344	34.8
Ce	35.4	47.9	57	54.4	52.3	124	151	86.2	105	133	448	114	128	742	71.9
Nd	25	32.8	41.4	38.9	38.5	67.5	85.3	51.3	57.9	71.6	194	61.6	71.4	290	41.8
Sm	8.1	10.3	13.2	11.7	12.1	16.5	20.1	13.3	15	18.8	39.8	14.4	18.1	52.5	10.4
Eu	2.9	3.5	4.4	4.1	4.1	5.1	6.3	4.2	4.7	5.8	9	4.6	5.4	3.8	3.2
Tb	1.9	2.5	3.4	2.8	2.7	2.5	3	2.2	2.6	2.9	5.5	2.5	2.8	6.5	1.9
Yb	4.4	5.8	7.5	7.5	7.4	5.1	6.3	4.7	5	6.1	10.7	5	6.6	11.6	3.9
Lu	0.7	1	1.3	1.2	1.3	0.8	1	0.7	0.8	0.9	1.7	0.8	1	1.7	0.6
Cr	572	542	518	479	509	154	231	373	421	398	548	223	247	54.3	394
Ni	129	186	158	166	154	67.5	110	105	132	125	167	68.4	94.4	39.8	99.8
V	1034	806	821	899	776	612	853	536	710	814	535	689	745	177	499
Cu	62.4	340	233	311	366	90.7	143	93.2	124	175	139	91.2	140	72.4	137
Co	81.1	118	104	109	96.3	71.7	110	86.2	92.1	98.1	57.3	52.4	71.4	23.5	55.7
Pb	12.5	12.6	15.5	15.5	13.8	14.8	22	14	18.4	18.6	52.3	18.2	17.9	59.7	16.2
Zn	183	209	220	241	256	198	344	228	218	257	207	198	235	235	179
Sn	7.9	9.6	8.5	9.1	8.3	7	9.9	7.7	8.9	8.7	11	6.2	7.7	9.2	5.8
Nb	11.4	14.6	17.6	18.4	17.3	38	41.3	28	34.2	37.1	122	27.4	33.2	123.1	25.5
Zr	200	219	280	269	275	506	633	396	447	530	1419	410	510	1122	383
Y	52	70.6	88.1	75.1	79.8	76	90.8	55.9	65.8	79.5	129	79.8	79.1	125	58
Rb	64.5	12.3	12.2	9.8	7.2	73.9	17.1	69.9	20.3	8.7	227	171	61.2	150	278
Sr	499	554	622	622	605	928	1513	1188	1420	1458	1643	570	1046	143	1346
Th	2.3		4.1	3.4	6.1	9.3	7.7	4.7	6	8.7	20.4	9.8	9.7	48.9	7.2
Ba	129	171	223	218	135	612	660	722	579	504	896	570	536	43.4	742

Table T13 (continued).

Hole:	183-1138A-												
Core, section:	78R-1	80R-4	81R-1	81R-2	82R-2	82R-5	83R-4	83R-5	84R-5	86R-3	87R-2	88R-2	88R-2
Interval (cm):	60–64	35–40	34–39	51–57	76–81	19–23	19–24	106–109	20–25	72–74	76–81	47–53	91–96
Piece:		2A	4A	2A	9	4	1	9	1C	8	13	2A	4
Lab number:	Z-1018	Z-1019	Z-1020	Z-1021	Z-1022	Z-1023	Z-1024	Z-1025	Z-1026	Z-1029	Z-1031	Z-1032	Z-1033
Depth (mbsf):	727.6	751.05	756.24	757.82	767.86	771.73	779.7	781.99	790.03	807.82	815.92	825.28	825.72
Major elements (g/1000 cm^3):													
Si	431	565	549	571	625	554	599	508	598	553	539	434	496
Ti	8.4	31.2	27.9	33.1	31.9	35	35.5	26.9	31	34	38	31.6	38.8
Al	105	201	173	196	152	170	186	168	198	170	169	118	152
Fe (sum)	85.1	248	215	237	223	258	276	203	278	299	310	209	302
Mn	0.6	3.9	2.5	5.3	2.4	4.9	5	2.1	6.6	6.7	9.1	4	6
Mg	17.5	101	92.2	94.4	81.2	95.4	95.1	86.3	98.1	84.9	87.4	67.8	83.5
Ca	29.3	171	152	200	142	186	200	157	198	135	154	118	136
Na	26	51.7	46.6	51.4	43.1	52.1	57.3	48.3	57	76.6	53.9	41.8	51.2
K	13.5	5	17.2	8.5	33.4	4	4.7	7.9	6.4	7.8	11.4	21.1	11.6
P	1	2.4	2.2	2.3	1.8	2.7	3.2	2.7	3.2	3.6	4.2	2.1	3.8
Minor elements (g/1000 $cm^3 \times 10^{-3}$):													
La	68.6	25	28.1	30.4	34.6	31.7	39.3	35.2	42.1	44.8	63.7	56.8	80.2
Ce	146	60	53.8	68.3	69.2	73.2	83.8	83.6	108	115	132	135	185
Nd	74.5	37.5	35.1	40.5	39.5	43.9	49.8	52.8	63.1	67.2	83.3	78.4	112
Sm	16.1	9.3	9.1	11.4	10.9	11.7	13.9	14.3	15.8	18.9	23.8	21.6	29.8
Eu	2.9	3.5	3.3	4	3.5	3.9	4.2	4.2	5.3	6	6.9	5.1	7.3
Tb	3.4	2.1	1.9	2.4	2.5	2.4	2.6	2.6	2.9	3.5	3.7	3.3	4.4
Yb	10.1	5.8	6.1	8.1	7.2	8.1	10	7.5	8.4	10.2	12.3	11.8	14
Lu	1.6	1	1	1.3	1.1	1.3	1.6	1.2	1.3	1.6	1.9	1.8	2.1
Cr	43.8	245	187	248	156	178	231	198	168	127	85.8	58.8	68.7
Ni	43.8	145	145	167	93.9	137	139	123	129	92	93.1	70.6	87
V	258	925	948	1341	709	1074	1035	1071	1091	884	1193	843	1138
Cu	86.1	400	339	342	346	415	445	297	395	610	466	510	561
Co	29.2	103	93.6	121	61.8	117	115	110	116	102	123	66.6	103
Pb	14.6		14	15.2	12.4	17.1	15.7	15.4	15.8	17.4	14.7	13.7	18.3
Zn	128	198	206	271	205	264	320	238	323	304	355	251	389
Sn	7.3	9.5	7	9.6	4.7	9.5	11	9.7	8.9	6.7	8.6	5.9	11.7
Nb	58.4	23.5	22.2	25.3	27.2	29.3	31.4	30.8	34.2	44.8	49	43.1	43.5
Zr	438	300	257	304	321	366	419	374	447	573	564	510	573
Y	78.8	60	70.2	75.9	79	87.8	105	90.2	103	112	123	112	133
Rb	58.4	10.5	23.4	11.1	56.8	4.6	3.7	11.4	2.9	11.2	13.2	41.2	17.9
Sr	788	525	1100	519	914	537	524	572	552	473	564	1196	435
Th	10.8	4.5		4		5.1		2.6	6	5.5	5.6	3.3	7.8
Ba	146	205	208	195	217	107	91.7	123	216	115	85.8	314	140

Table T13 (continued).

Hole:	183-1140A-													
Core, section:	27R-1	27R-1	27R-2	31R-1	31R-1	32R-3	32R-4	34R-1	34R-3	35R-1	35R-1	36R-4	37R-1	37R-2
Interval (cm):	17–27	63–67	78–83	9–13	76–79	5–10	17–20	117–121	100–105	35–42	83–87	61–67	93–99	55–60
Piece:	1A	4	3B	1	5	2	2	4D	3	2A	4	2D	1D	2A
Lab number:	Z-1034	Z-1035	Z-1036	Z-1037	Z-1038	Z-1039	Z-1040	Z-1041	Z-1042	Z-1043	Z-1044	Z-1045	Z-1046	Z-1047
Depth (mbsf):	239.47	239.93	241.49	270.59	271.26	278.25	279.83	295.27	297.78	303.85	304.33	317.52	318.23	318.97
Major elements (g/1000 cm^3):														
Si	657	647	637	598	632	589	644	585	580	656	665	678	657	660
Ti	21.5	19.5	19.6	33	37.2	49.2	19.2	18.2	17.6	23.9	22.8	21.3	21.1	18.8
Al	231	224	223	221	220	187	235	216	222	231	222	225	227	43.91
Fe (sum)	265	267	262	217	230	249	232	220	185	279	245	247	224	257
Mn	1.1	4.1	3.6	3.7	3.7	2.6	2.3	3.3	1.8	3.2	3.2	3	3.1	3.9
Mg	116	127	144	88.3	97.9	85.51	115	115	132	120	107	139	109	115
Ca	250	248	233	213	215	177	220	199	192	250	256	251	247	258
Na	55.9	57	56.4	55.4	61.9	59.7	57	51	51.5	59.8	61.2	61.8	60	60.6
K	3.2	10.8	2.7	12.9	8.3	11.3	19.6	1.8	7.9	11	12.4	2.8	2.6	3.9
P	1.6	1.4	7.5	3.4	2.8	3.9	1.7	1.3	1.3	1.5	1.5	1.6	1.5	1.7
Minor elements (g/1000 cm^3 × 10^{-3}):														
La	11	11.8	10.7	34.1	38.2	130.1	32	10	9.3	11.7	12.3	11.5	12.9	12.7
Ce	23.8	31.8	28.8	83.8	90.1	318.6	88.1	24.2	28.3	32.2	37.3	35.4	39.2	37.4
Nd	24.7	28.9	25.9	55	57.3	195.1	67.3	21.1	21.6	28.1	28.7	26.6	30.8	31.7
Sm	10.4	11	10.1	15.5	14.7	54.6	22.4	7.7	7.7	10.5	10	9.1	9.5	9.8
Eu	3.8	3.8	3.7	5.2	5.5	16.9	9.6	2.8	2.8	3.8	4	3.8	3.6	3.7
Tb	2.4	2.8	2.5	2.6	3.3	9.1	6.7	1.9	2.1	2.8	2.4	2.5	2.4	2.4
Yb	8.1	8.1	7.2	7.3	7.9	22.8	19.2	6.2	5.9	7.9	7.5	6.5	7	7.5
Lu	1.2	1.1	1.1	1	1.1	3	3	1	1	1.3	1.3	1	1.1	1.2
Cr	769	795	850	270	410	436	2162	707	822	498	517	590	504	576
Ni	267	243	294	128	199	299	833	216	247	190	132	189	185	236
V	885	858	893	917	1016	2581	2819	969	900	929	1010	994	1014	1071
Cu	493	405	461	354	396	943	1682	411	398	498	474	502	518	533
Co	145	107	170	94.32	128	273	400	159	139	144	112	159	154	184
Pb	17	14	14	16	16	39	40	12.9	15.4	17.6	14.4	17.7	16.8	14.4
Zn	270	254	268	267	437	891	737	239	234	226	287	274	272	288
Sn	9.86	9.83	7.2	8.91	8.19	24.71	20	9.25	9	9.7	9.5	10.6	10.6	8.6
Nb	10.4	7.8	10.4	7.9	30	84.5	160.2	10	5.4	10.5	11.2	7.4	12	11.2
Zr	234.9	225	225	199	437	1105	1842	185	164	226	221	221	218	219
Y	84.1	92.5	83.5	83.8	90.1	280	208	66.8	64.3	85	89	82.6	78.4	80.6
Rb		26.6	4.3	20.7	6.8	37.1	96.1		12.6	26.4	26.7			3.2
Sr	377	376	346	655	710	1626	881	283	283	352	344	384	336	346
Th		2.9	3.2	3.7	5.2	15	12.8				4	3.5		
Ba	157	83.8	138	244	328	975	88.1	123	69.4	82.0	106	133	81.2	89.3

Table T14. Mass balance at low-temperature alteration of the basalts from the Kerguelen Plateau.

Core, section, interval (cm)	Description	H_2O^+ (wt%)	Density (g/cm^3)	Major elements (g/1000 cm^3)													
				Si	Al	Fe	Mn	Mg	Ca	Na	K	P	Ni	V	Cu	Co	Zn
Nonoxidizing alteration:																	
183-1140A-																	
35R-1, 35–42*	Nonaltered basalt	0.74	2.93	656	231	279	3.2	120	250	59.8	11	1.5	190	929	498	144	226
34R-1, 117–121	Altered basalt	1.40	2.57	585	216	220	3.3	115	199	51.0	1.8	1.3	216	969	411	159	239
Percent difference between altered and nonaltered basalt:				–10.8	–6.5	–21.1	+3.1	–4.2	–20.4	–14.7	–83.6	–13.3	+13.7	+4.3	–17.5	+10.4	+5.7
Oxidizing alteration:																	
183-1137A-																	
39R-2, 114–119*	Nonaltered basalt	0.99	2.28	578	178	168	4.8	71.2	43.7	57.0	105	3.3	68.4	689	91.2	52.4	198
27R-1, 100–105	Altered basalt	2.03	2.11	493	163	173	1.9	84.7	61	52.5	55.1	3.5	67.5	612	90.7	71.7	198
Percent difference between altered and nonaltered basalt:				–14.7	–8.4	+3.0	–60.4	+19.0	+39.6	–7.9	–47.5	+6.0	–1.3	–11.2	–0.5	+2.6	0

Note: * = abundance of elements for nonaltered basalt.

Table T14 (continued).

Core, section, interval (cm)	Description	H_2O^+ (wt%)	Density (g/cm^3)	Minor elements (g/1000 cm^3 × 10^{-3})															
				Nb	Zr	Y	Rb	Sr	Ba	La	Ce	Nd	Sm	Eu	Tb	Yb	Lu	H_2O^+	d_v
Nonoxidizing alteration:																			
183-1140A-																			
35R-1, 35–42*	Nonaltered basalt	0.74	2.93	10.5	226	85	26.4	352	82	11.7	32.2	28.1	10.5	3.8	2.8	7.9	1.3	0.74	2.93
34R-1, 117–121	Altered basalt	1.40	2.57	10.0	185	66.8		283	123	10.0	24.2	21.1	7.7	2.8	1.9	6.2	1.0	1.40	2.57
Percent difference between altered and nonaltered basalt:				–4.8	–18.1	–21.4		–19.6	+50.0	–14.5	–24.8	–24.9	–26.7	26.3	–32.1	–21.5	–23.0		
Oxidizing alteration:																			
183-1137A-																			
39R-2, 114–119*	Nonaltered basalt	0.99	2.28	27.4	410	79.8	171	570	570	57	114	61.6	14.4	4.6	2.5	5.0	0.8	0.99	2.28
27R-1, 100–105	Altered basalt	2.03	2.11	38.0	506	76.0	73.9	928	612	57	124	67.5	16.5	5.1	2.5	5.1	0.8	2.03	2.11
Percent difference between altered and nonaltered basalt:				–38.7	+23.4	–4.8	–56.8	+62.8	+7.4	0	+8.8	+9.6	+14.6	+10.7	0	+2.0	0		